PRINCIPLES OF COMPOSITE MATERIAL MECHANICS

SECOND EDITION

Extensively revised and maintaining the high standard of the popular original, **Principles of Composite Materials Mechanics, Second Edition** reflects the many recent developments in the mechanics of composite materials. New and up-to-date information throughout the text brings modern engineering students everything they need to advance their knowledge of the ever more common composite materials.

The introduction strengthens the book's emphasis on fundamental principles of mechanics by adding a review of the basic mechanics of materials equations. New appendices cover the derivations of stress equilibrium equations and the strain–displacement relations from elasticity theory. Additional sections address recent applications of composite mechanics to nanocomposites, composite grid structures, and composite sandwich structures. More detailed discussion of elasticity and finite element models have been included along with results from the recent World Wide Failure Exercise. A phenomenological approach is taken to illustrate linear viscoelastic behavior of composites. Updated information on the nature of fracture and composite testing includes coverage of the finite element implementation of the Virtual Crack Closure technique and new and revised ASTM standard test methods. The author includes updated and expanded material property tables, many more example problems and homework exercises, as well as new reference citations throughout the text.

DK2140

ISBN 0-8247-5389-5
90000
9 780824 753894

www.crcpress.com

RC Press
or & Francis Group
iforma business
v.taylorandfrancisgroup.com

6000 Broken Sound Parkway, NW
Suite 300, Boca Raton, FL 33487
270 Madison Avenue
New York, NY 10016
2 Park Square, Milton Park
Abingdon, Oxon OX14 4RN, UK

Gibson

PRINCIPLES OF COMPOSITE MATERIAL MECHANICS

SECOND EDITION

COMPOSITE MATERIAL MECHANICS

SECOND EDITION

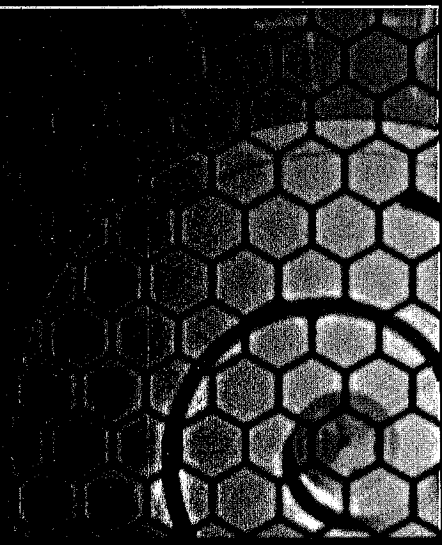

Ronald F. Gibson

CRC Press
Taylor & Francis Group

About the Author

Ronald F. Gibson is a professor of mechanical engineering and director of the Advanced Composites Research Laboratory at Wayne State University. Dr. Gibson received his B.S. degree in mechanical engineering from the University of Florida, his M.S. in mechanical engineering from the University of Tennessee, and his Ph.D. in mechanics from the University of Minnesota. He has held full-time faculty positions at Iowa State University, the University of Idaho, and Wayne State University, and visiting faculty positions at Stanford University, the University of Florida, and Michigan State University. He has been a development engineer for Union Carbide Corporation and a summer faculty fellow at the NASA Langley Research Center.

Dr. Gibson is an active member of numerous professional societies, including the American Society of Mechanical Engineers, the American Society for Composites, the American Society for Testing and Materials, the Society for Experimental Mechanics, and the Society for the Advancement of Material and Process Engineering. He has served the American Society for Composites as its president, vice-president, and membership secretary. He has been the recipient of the Hetenyi Award for Best Research Paper of the Year from the Society for Experimental Mechanics, the College of Engineering Outstanding Faculty Award from the University of Idaho, the Distinguished Faculty Fellowship Award, the Devlieg Professorship, and the Outstanding Graduate Faculty Mentor Award from Wayne State University. He is an elected Fellow of the American Society of Mechanical Engineers and the American Society for Composites. The results of his research have been published in numerous scholarly articles and presented at a variety of national and international meetings.

Contents

Preface to First Edition

Composite materials is truly an interdisciplinary subject, and the number of students taking courses in this area is steadily increasing. Books on the subject tend to emphasize either the mechanics or the materials science aspects of composites. *Principles of Composite Material Mechanics* is mechanics oriented. Composite materials technology is new enough for many working engineers to have had no training in this area, so a textbook in composite material mechanics should be useful not only for the education of new engineers, but also for the continuing education of practicing engineers and for reference. The high level of interest in composite materials, the interdisciplinary nature of the subject, the need to re-educate practicing engineers, and the need for a new composite mechanics textbook at the introductory level all led to my decision to write this book.

Chapters 1 through 7 form the basis of a one-semester senior/graduate-level course in mechanical engineering, which I have taught for the last 15 years. Chapters 8 through 10, along with selected papers from technical journals and student research projects/presentations, form the basis of a second one-semester course, which is taken only by graduate students, and which I have taught for the last four years. The book could also be the basis for a two-quarter sequence by omitting some topics. Prerequisities for the course are knowledge of mechanics of materials, introduction to materials engineering, and ordinary differential equations, and previous exposure to linear algebra is highly desirable. For some of the graduate-level material, earlier courses in advanced mechanics of materials, elasticity, and partial differential equations are recommended, but not required.

Some of the basic elements of composite mechanics covered in this book have not changed since the first books on the subject were published in the 1960s and 1970s, and, where possible, I have tried to use the accepted terminology and nomenclature. For example, the coverage of stress–strain relationships and transformation of properties for anisotropic materials in Chapter 2 and the classical lamination theory in Chapter 7 is consistent with that of previous textbooks such as the *Primer on Composite Materials* by Ashton, Halpin, and Petit, and *Mechanics of Composite Materials* by Jones. However, rather than beginning the study of laminates by jumping directly into classical lamination theory, I have concluded that a better pedagogical approach is to introduce first basic laminate concepts by

using the simpler theory of laminated beams in pure flexure. Also, I believe that the concept of an effective modulus of an equivalent homogeneous material, which had previously been covered only in advanced books such as *Mechanics of Composite Materials* by Christensen, is essential for the proper development of heterogeneous composite micromechanics. Thus, effective modulus concepts are emphasized from their introduction in Chapter 2 to their use in the analysis of viscoelastic and dynamic behavior in Chapter 8.

Although many basic concepts have been presented in earlier textbooks, numerous new developments in composite mechanics over the last two decades have made it increasingly necessary to supplement these books with my own notes. Thus, I have added coverage of such important topics as hygrothermal effects in Chapter 5, discontinuous fiber composites in Chapter 6, viscoelastic behavior and dynamic behavior in Chapter 8, fracture in Chapter 9, and mechanical testing in Chapter 10. The coverage of experimental mechanics of composites has been expanded to include summaries of the most important ASTM standard test methods, many of which did not exist when the early mechanics of composites books were published. A variety of example problems and homework problems, a number of them related to practical composite structures, are also included.

The contents of this book represent the cumulative effects of more than 25 years of interactions with colleagues and students, and I would be remiss if I did not mention at least some of them. My fascination with composites began in 1965 with my first engineering position in what is now part of Oak Ridge National Laboratory in Tennessee, where I was involved in the design and development of high-speed rotating equipment. At that time I realized that the advantages of using composites in rotating equipment are numerous, as is the case in many other applications. My experiences working with Dean Waters and other colleagues in the mechanical development group in Oak Ridge have had a strong influence on my later career decision to emphasize composites research and education. My doctoral research on vibration damping characteristics of composites with Robert Plunkett at the University of Minnesota further cemented my desire to continue working in the composites area and ultimately led to my career in university teaching and research.

After beginning my academic career at Iowa State University in 1975, I began a long and productive association with C.T. Sun, and later had the pleasure of spending a one-year leave working with C.T. and his colleagues Robert Sierakowski and Shive Chaturvedi at the University of Florida. I owe much of my understanding of composite mechanics to interactions with them. The notes leading to this book were developed by teaching composite mechanics courses at Iowa State University, the University of

Idaho, the University of Florida, Michigan State University, and Wayne State University, and I am indebted to the students who took my classes and helped me to "debug" these notes over the years. Most recently, my students at Wayne State University have been particularly effective at finding the inevitable errors in my notes. Interaction with my graduate students over the years has contributed immeasurably to my understanding of composite mechanics, and the work of several of those students has been referred to in this book. I am particularly indebted to Stalin Suarez, Lyle Deobald, Raju Mantena, and Jimmy Hwang, all former graduate students at the University of Idaho.

Serious work on this book actually began during a sabbatical leave at Michigan State University in 1987, and I am indebted to Larry Drzal and his colleages for our many stimulating discussions during that year. Particularly important was the interaction with Cornelius Horgan, with whom I team-taught a course on advanced mechanics of composites. Most recently, my collaboration with John Sullivan and his colleagues of the Ford Scientific Research Laboratory has proved to be very rewarding, and I am indebted to John for his careful review of the manuscript and helpful comments. I am grateful to Carl Johnson, also of the Ford Scientific Research Laboratory, for his encouragement and support and for providing several of the figures in Chapter 1. The strong support of Wayne State University, which made it possible to establish the Advanced Composites Research Laboratory there in 1989, is gratefully acknowledged. The support and encouragement of my department chairman, Ken Kline, has been particularly important. Generous support for my composites research from numerous funding agencies over the years has also helped to make this book possible. Grants from the Air Force Office of Scientific Research, the National Science Foundation, the Army Research Office, the Boeing Company, and the Ford Motor Company have been particularly important.

McGraw-Hill and I would like to thank the following reviewers for their many helpful comments and suggestions: Charles W. Bert, University of Oklahoma; Olivier A. Bauchau, Rensselaer Polytechnic Institute; Shive Chaturvedi, Ohio State University; Vincent Choo, New Mexico State University; John M. Kennedy, Clemson University; Vikram K. Kinra, Texas A & M University; C.T. Sun, University of Florida; and Steven W. Yurgartis, Clarkson University.

Finally, my wife and best friend, Maryanne, has been my strongest supporter as I labored on this project, and there is no way that I could have done it without her love, encouragement, patience, and understanding.

Ronald F. Gibson

Preface

There have been many developments in mechanics of composite materials since the first edition of this book was published. Accordingly, the second edition has new sections on recent applications of composite mechanics to nanocomposites, composite grid structures, and composite sandwich structures. To strengthen the emphasis on the basic principles of mechanics, I have added a review of the basic mechanics of materials equations in the Introduction, and appendices covering the derivations of stress equilibrium equations and strain–displacement relations from elasticity theory. Coverage of micromechanics in Chapter 3 has been revised to include more detailed discussions of elasticity and finite element models. Chapter 4 on strength analysis has been updated to include results from the World Wide Failure Exercise. Chapter 8 has been improved by adding a phenomenological approach to understanding linear viscoelastic behavior of composites. Chapter 9 on fracture has been updated to include coverage of the finite element implementation of the virtual crack closure technique. Chapter 10 on testing of composites and their constituents has been extensively updated to include coverage of both new and revised ASTM standard test methods. Finally, more example problems and homework problems have been added to most chapters, and new references have been cited throughout.

As with the first edition, I am indebted to many colleagues, graduate students, and sponsors. I am grateful to Wayne State University for providing a nurturing environment for my teaching and research, and for granting me sabbatical leaves, which were essential to the completion of this project. My graduate students have been particularly helpful in identifying the inevitable errors in the first edition, and their thesis research findings have enabled me to add important new dimensions in the second edition. And as with the first edition, my wife and best friend, Maryanne, has continued to be my strongest supporter, and I will be forever grateful for her love, encouragement, patience, and understanding.

Ronald F. Gibson

1

Introduction

1.1 Basic Concepts

Structural materials can be divided into four basic categories: metals, polymers, ceramics, and composites. Composites, which consist of two or more separate materials combined in a structural unit, are typically made from various combinations of the other three materials. In the early days of modern man-made composite materials, the constituents were typically macroscopic. As composites technology advanced over the last few decades, the constituent materials, particularly the reinforcement materials, steadily decreased in size. Most recently, there has been considerable interest in "nanocomposites" having nanometer-sized reinforcements, such as carbon nanotubes.

The relative importance of the four basic materials in a historical context has been presented by Ashby [1], as shown schematically in figure 1.1 that clearly shows the steadily increasing importance of polymers, composites, and ceramics and the decreasing role of metals. Composites are generally used because they have desirable properties that cannot be achieved by any of the constituent materials acting alone. The most common example is the fibrous composite consisting of reinforcing fibers embedded in a binder or matrix material. Particle or flake reinforcements are also used, but they are generally not so effective as fibers.

Although it is difficult to say with certainty when or where humans first learned about fibrous composites, nature provides us with numerous examples. Wood consists mainly of fibrous cellulose in a matrix of lignin, whereas most mammalian bone is made up of layered and oriented collagen fibrils in a protein–calcium phosphate matrix [2]. The book of Exodus in the *Old Testament* recorded what surely must be one of the first examples of man-made fibrous composites, the straw-reinforced clay bricks used by the Israelites. The early natives of South and Central America apparently used plant fibers in their pottery. These early uses of fibrous reinforcement, however, were probably based on the desire to keep the clay from cracking during drying rather than on structural reinforcement. Much later, humans developed structural composites such

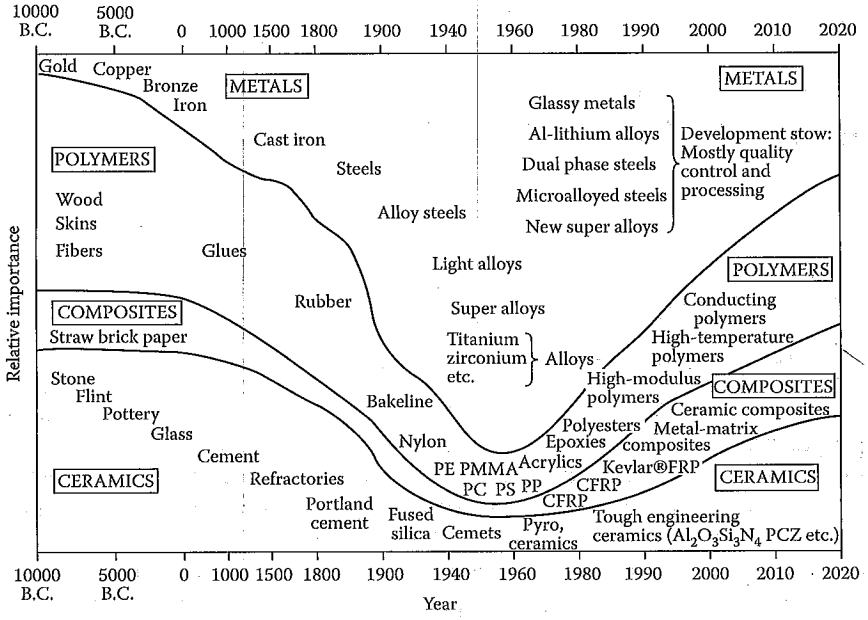

FIGURE 1.1
The relative importance of metals, polymers, composites, and ceramics as a function of time. The diagram is schematic and describes neither tonnage nor value. The time scale is nonlinear. (From Ashby, M.F. 1987. *Philosophical Transactions of the Royal Society of London*, A322, 393–407. With permission.)

as steel-reinforced concrete, polymers reinforced with fibers such as glass and graphite, and many other materials.

Fibrous reinforcement is so effective because many materials are much stronger and stiffer in fiber form than in bulk form. It is believed that this phenomenon was first demonstrated scientifically in 1920 by Griffith [3], who measured the tensile strengths of glass rods and glass fibers of different diameters. Griffith found that as the rods and fibers got thinner, they got stronger (see fig. 1.2 from ref. [3], as shown in ref. [4]), apparently because the smaller the diameter, the smaller the likelihood that failure-inducing surface cracks would be generated during fabrication and handling. By extrapolating these results, Griffith found that for very small diameters, the fiber strength approached the theoretical cohesive strength between adjacent layers of atoms, whereas for large diameters, the fiber strength dropped to near the strength of bulk glass.

Results similar to those published by Griffith have been reported for a wide variety of other materials. The reasons for the differences between

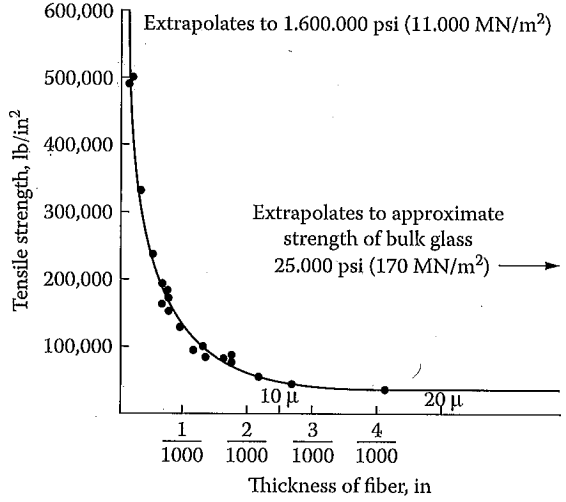

FIGURE 1.2
Griffith's measurements of tensile strength as a function of fiber thickness for glass fibers. (Data from Griffith, A.A. 1920. *Philosophical Transactions of the Royal Society*, 221A, 163–198, as analyzed by Gordon, J.E. 1976. *The New Science of Strong Materials*, 2d ed. [Princeton University Press, Princeton, NJ]. With permission.)

fiber and bulk behavior, however, are not necessarily the same for the other materials. For example, polymeric fibers are stronger and stiffer than bulk polymers because of the highly aligned and extended polymer chains in the fibers and the randomly oriented polymer chains in the bulk polymer. A similar effect occurs in crystalline materials such as graphite. In addition, a single crystal tends to have a lower dislocation density than a polycrystalline solid; so single-crystal "whisker" materials are much stronger than the same material in polycrystalline bulk form. Whiskers typically have dimensions in the micrometer range, and for many years it was thought that whiskers were the strongest and stiffest reinforcement materials available. However, it is now believed that carbon nanotubes, which have dimensions in the nanometer range, are the strongest and stiffest reinforcement materials in existence [5,6].

There can be no doubt that fibers allow us to obtain the maximum tensile strength and stiffness of a material, but there are obvious disadvantages of using a material in fiber form. Fibers alone cannot support longitudinal compressive loads and their transverse mechanical properties are generally not so good as the corresponding longitudinal properties. Thus, fibers are generally useless as structural materials unless they are held together in a structural unit with a binder or matrix material and unless some

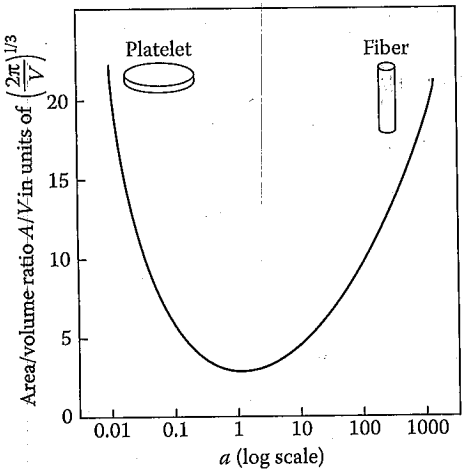

FIGURE 1.3
Surface area-to-volume ratio A/V of a cylindrical particle of given volume plotted vs. particle aspect ratio $a = l/d$. (From McCrum, N.G., Buckley, C.P., and Bucknall, C.B. 1988. *Principles of Polymer Engineering* [Oxford University Press, New York]. Copyright 1988, Oxford University Press with permission.)

transverse reinforcement is provided. Fortunately, the geometrical configuration of fibers also turns out to be very efficient from the point of view of interaction with the binder or matrix. As shown in figure 1.3 from ref. [7], the ratio of surface area to volume for a cylindrical particle is greatest when the particle is in either platelet or fiber form. Thus, the fiber/matrix interfacial area available for stress transfer per unit volume of fiber increases with increasing fiber length-to-diameter ratio. The matrix also serves to protect the fibers from external damage and environmental attack. Transverse reinforcement is generally provided by orienting fibers at various angles according to the stress field in the component of interest. Filler particles are also commonly used in composites for a variety of reasons such as weight reduction, cost reduction, flame and smoke suppression, and prevention of ultraviolet degradation due to exposure to sunlight.

The need for fiber placement in different directions according to the particular application has led to various types of composites, as shown in figure 1.4. In the continuous fiber composite laminate (fig. 1.4[a]), individual continuous fiber/matrix laminae are oriented in the required directions and bonded together to form a laminate. Although the continuous fiber laminate is used extensively, the potential for delamination, or separation of the laminae, is still a major problem because the interlaminar

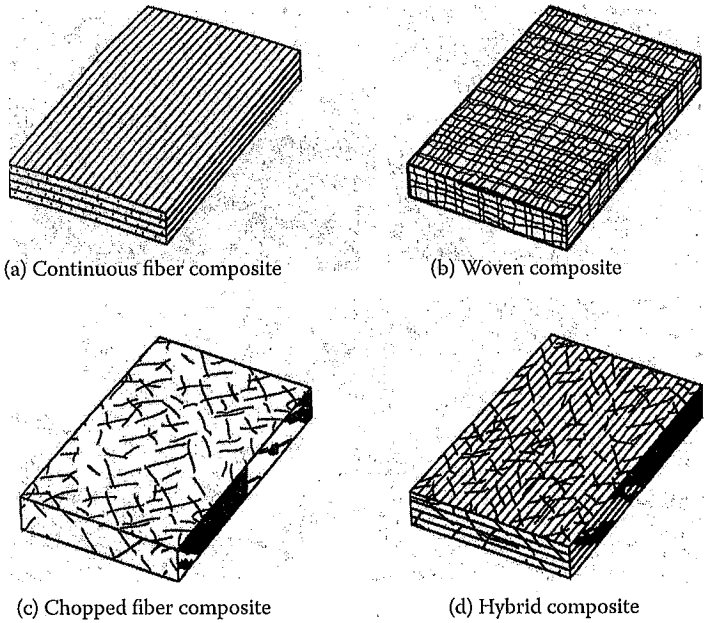

FIGURE 1.4
Types of fiber-reinforced composites.

strength is matrix dominated. Woven fiber composites (fig. 1.4[b]) do not have distinct laminae and are not susceptible to delamination, but strength and stiffness are sacrificed because the fibers are not so straight as in the continuous fiber laminate. Chopped fiber composites may have short fibers randomly dispersed in the matrix, as shown in figure 1.4(c). Chopped fiber composites are used extensively in high-volume applications due to their low manufacturing cost, but their mechanical properties are considerably poorer than those of continuous fiber composites. Finally, hybrid composites may consist of mixed chopped and continuous fibers, as shown in figure 1.4(d), or mixed fiber types such as glass and graphite. Another common composite configuration, the sandwich structure (fig. 1.5), consists of high-strength composite facing sheets (which could be any of the composites shown in fig. 1.4) bonded to a lightweight foam or honeycomb core. Sandwich structures have extremely high flexural stiffness-to-weight ratios and are widely used in aerospace structures. The design flexibility offered by these and other composite configurations is obviously quite attractive to designers, and the potential exists to design not only the structure but also the structural material itself.

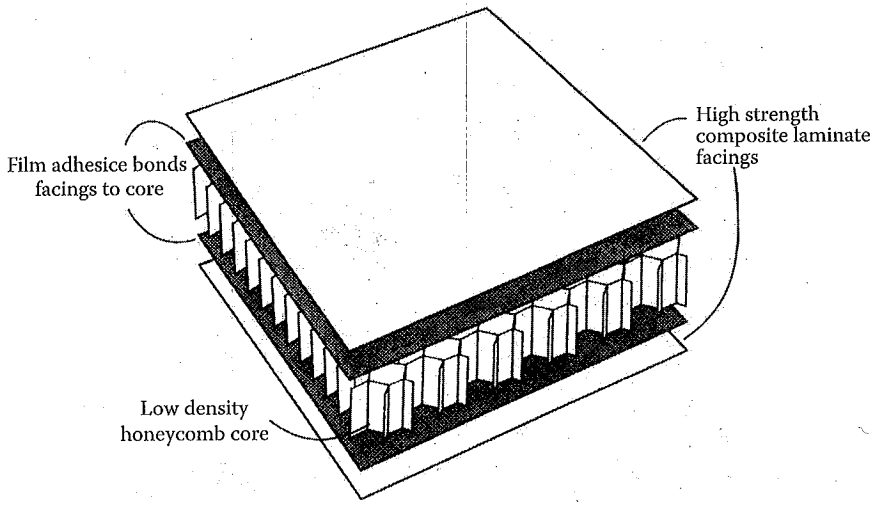

FIGURE 1.5
Composite sandwich structure.

1.2 Constituent Materials for Composites

Fiberglass-reinforced plastics were among the first structural composites. Composites incorporating glass or other relatively low-modulus fibers (less than about 83 GPa (12×10^6 psi) are used in many high-volume applications such as automotive vehicles because of their low cost, and are sometimes referred to as "basic" composites. The so-called "advanced" composites made from carbon, silicon carbide, aramid polymer, boron, or other higher-modulus fibers are used mainly in more exotic applications such as aerospace structures where their higher cost can be justified by improved performance.

The tremendous advantages of advanced fibers over glass fibers and conventional bulk materials are shown in table 1.1, by comparing selected properties. The main advantages are higher modulus, higher strength, and lower density. In many applications such as aerospace and automotive structures, structural weight is very important. Depending on whether the structural design is strength-critical or stiffness-critical, the material used should have a high strength-to-weight ratio (or specific strength) or a high stiffness-to-weight ratio (or specific stiffness). As shown in figure 1.6, advanced fibers also have significant advantages over conventional materials in both these measures, and this is the principal

TABLE 1.1
Selected Properties of Bulk and Fibrous Materials

Material	Tensile Strength (MPa)	Tensile Modulus (GPa)	Density (g/cm³)	Specific Strength (MPa/[g/cm³])	Specific Modulus (GPa/[g/cm³])	Ultimate Strain	Manufacturer
Bulk Metals							
6061T6 Aluminum	310	69	2.71	114.4	25.5	0.17	
4340 Steel	1030	200	7.83	131.5	25.5	0.19	
AZ80 Magnesium	345	45	1.8	191.7	25	0.06	
Bulk Polymers							
Nylon 6/6	75	2.8	1.14	65.8	2.5	0.5	
Polycarbonate	65	2.4	1.2	54.2	2	1.1	
Polyvinylchloride	40	3.1	1.44	27.8	2.2	0.4	
Bulk Ceramics							
Silicon carbide	0.4	400	3.4	0.1	117.6	0.001	
Aluminum oxide	0.5	380	3.8	0.1	100	0.001	
Glass Fibers							
E-glass	3448	72	2.54	1357.5	28.3	0.04	Owens-Corning
S-2 glass	4830	87	2.49	1939.8	34.9	0.057	Owens-Corning
PAN-Based Carbon Fibers							
AS4	4278	228	1.79	2389.9	127.4	0.0187	Hexcel
IM7	5175	276	1.78	2907.3	155.1	0.0178	Hexcel

(Continued)

TABLE 1.1 (CONTINUED)
Selected Properties of Bulk and Fibrous Materials

Material	Tensile Strength (MPa)	Tensile Modulus (GPa)	Density (g/cm³)	Specific Strength (MPa/[g/cm³])	Specific Modulus (GPa/[g/cm³])	Ultimate Strain	Manufacturer
PAN-Based Carbon Fibers (Continued)							
IM9	6072	290	1.8	3373.3	161.1	0.018	Hexcel
T-300	3750	231	1.76	2130.7	131.3	0.014	Cytec
T-650/35	4280	255	1.77	2418.1	144.1	0.017	Cytec
T-800S	5880	294	1.8	3266.7	163.3		Toray
T-1000G	6370	294	1.8	3538.9	163.3		Toray
Pitch-Based Carbon Fibers							
P-55S	1900	379	1.9	1000	199.5	0.005	Cytec
P-100S	2410	758	2.16	1115.7	350.9	0.003	Cytec
P-120S	2410	827	2.17	1110.6	381.1	0.003	Cytec
Polymeric Fibers							
Kevlar 29 aramid	3620	83	1.44	2513.9	57.6	0.044	DuPont
Kevlar 49 aramid	3792	131	1.44	2633.3	91	0.023	DuPont
Spectra 900/650 polyethylene	2400	66	0.97	2474.2	68	0.041	Honeywell
Spectra 2000/100 polyethylene	3340	124	0.97	3443.3	127.8	0.03	Honeywell
Technora aramid	3430	73	1.39	2467.6	52.5	0.046	Teijin
Zylon-AS PBO	5800	180	1.54	3766.2	116.9	0.035	Toyobo
Other Fibers							
Boron 4.0 mil dia	3516	400	2.57	1368.1	155.6	0.008	Specialty Materials
SCS-6 silicon carbide	3450	380	3	1150	126.7	0.0013	Specialty Materials
Carbon nanotubes	30000	1000	1.9	15789.5	526.3		

FIGURE 1.6
Specific modulus vs. specific strength for a variety of fibers and conventional bulk materials. The specific value is the value of the property divided by the density.

reason that composites will be used with increasing frequency in aerospace structures, fiber-reinforced automotive structures, and other structures where these properties are important. When the reinforcing fibers are combined with a matrix or binder material to form a composite, there is obviously some reduction in the tremendously high specific strengths and specific moduli shown for the reinforcing fibers in figure 1.6, but the composites still have an overwhelming advantage with respect to these properties. Table 1.1 also shows that the ultimate strain, or strain to failure (a measure of ductility), is one measure where reinforcing fibers are typically not as good as conventional bulk metals and polymers, but are still better than bulk ceramics. Many advanced fibers exhibit nearly linear stress–strain curves to failure, and such behavior is generally considered to be characteristic of brittle materials. It is important to remember, however, that the fiber strength, fiber modulus, and fiber ultimate strain values in Table 1.1 are based on tensile tests with the load acting along the fiber axis. As shown later, these properties all change substantially for off-axis loading, and applied loads are rarely aligned perfectly with the fiber axis. It will be shown later, for example, that a composite laminate can be constructed in such a way that its overall behavior is similar to that of ductile metals, even though the reinforcing fibers may exhibit brittle behavior.

1.2.1 Fiber Materials

Glass fibers consist primarily of silica (silicon dioxide) and metallic oxide–modifying elements and are generally produced by mechanical drawing of molten glass through a small orifice. E-glass (named for its electrical properties) accounts for most of the glass fiber production and is the most widely used reinforcement for composites. The second most popular glass fiber, S-glass, has roughly 40% greater tensile strength and 20% greater modulus of elasticity than E-glass (table 1.1), but it is not as widely used, because of its higher cost. S-glass actually has greater strength than many advanced fibers, but its relatively low modulus limits its application. Glass/epoxy and glass/polyester composites are used extensively in applications ranging from fishing rods to storage tanks and aircraft parts.

Graphite or carbon fibers are the most widely used advanced fibers, and graphite/epoxy or carbon/epoxy composites are now used routinely in aerospace structures. Unfortunately, the names "carbon" and "graphite" are often used interchangeably to describe fibers based on the element carbon. These fibers are usually produced by subjecting organic precursor fibers such as polyacrylonitrile (PAN) or rayon to a sequence of heat treatments, so that the precursor is converted to carbon by pyrolysis. The major difference is that graphite fibers are subjected to higher temperature pyrolysis than carbon fibers. The result is that carbon fibers typically are less than 95% carbon, whereas graphite fibers are at least 99% carbon [8]. Although carbon fibers were once prohibitively expensive, the cost has dropped significantly as production capacity and demand has increased. Development of new carbon and graphite fibers continues at a rapid pace. For example, fibers based on a pitch precursor (P-120S) with a modulus more than four times that of steel are now available (Table 1.1). High-strength carbon fibers such as T-1000G, which are based on a PAN precursor, have a tensile strength more than six times that of steel. Either high strength or high modulus is obtained by using the appropriate heat treatment.

Advanced polymeric fibers such as Kevlar® aramid fibers by DuPont, Spectra® polyethylene fibers by Honeywell, Technora® aramid fibers by Teijin, and Zylon® *para*-phenylene benzobisoxazole (PBO) fibers by Toyobo have extremely high specific strengths because of their combinations of high strength and low density. The polymeric fibers also have higher failure strains (i.e., better ductility) than the glass or carbon fibers. The main disadvantages of the polymeric fibers are that they are generally not suitable for use at extremely high temperatures, and some of them are also susceptible to moisture-induced degradation. The effects of temperature and moisture on polymers and polymer composites will be discussed in more detail in chapter 5.

Boron fibers are actually composites consisting of a boron coating on a

the largest of all the advanced fibers, typically 0.002 to 0.008 in (0.05 to 0.2 mm). Boron fibers have much higher moduli than most carbon fibers (table 1.1), but they also have higher density. Boron/epoxy and boron/aluminum composites are widely used in aerospace structures where high stiffness is needed, but high cost still prevents more widespread use.

Silicon carbide (SiC) fibers are used primarily in high-temperature metal and ceramic matrix composites because of their excellent oxidation resistance and high-temperature strength retention. At room temperature, the strength and stiffness of SiC fibers are about the same as those of boron. SiC whisker-reinforced metals are also receiving considerable attention as alternatives to unreinforced metals and continuous fiber-reinforced metals. SiC whiskers are very small, typically 8 to 20 μ in (20 to 51 nm) in diameter and about 0.0012 in (0.03 mm) long, so that standard metal-forming processes such as extrusion, rolling, and forging can be easily used [7].

The ultimate reinforcement material to date is the carbon nanotube. Carbon nanotubes, which were first observed in 1991, are two-dimensional hexagonal networks of carbon atoms (graphene sheets) that have been rolled up to form a cage-like hollow tube having a diameter of several nanometers [5,6]. The properties for nanotubes presented in table 1.1 are only approximate, as nanotubes have so many different possible configurations. For example, they can be single-walled or multi-walled, and they may occur in the form of bundles or ropes.

Hybrids consisting of mixed fiber materials can be used when a single fiber material does not have all the desired properties. More complete descriptions of fiber materials and their properties can be found in several composites handbooks [8–13]. Further discussion of fiber properties, including anisotropic behavior, will be given in chapter 3.

1.2.2 Matrix and Filler Materials

Polymers, metals, and ceramics are all used as matrix materials in composites, depending on the particular requirements. The matrix holds the fibers together in a structural unit and protects them from external damage, transfers and distributes the applied loads to the fibers, and in many cases contributes some needed property such as ductility, toughness, or electrical insulation. A strong interface bond between the fiber and matrix is obviously desirable, so the matrix must be capable of developing a mechanical or chemical bond with the fiber. The fiber and matrix materials should also be chemically compatible, so that undesirable reactions do not take place at the interface. Such reactions tend to be more of a problem in high-temperature composites. Service temperature is often the main consideration in the selection of a matrix material. Thus, the materials will be discussed below in order of increasing temperature capability.

Polymers are unquestionably the most widely used matrix materials in modern composites. Polymers are described as being either thermosets (e.g., epoxy, polyester, phenolic) or thermoplastics (e.g., polyimide [PI], polysulfone, polyetheretherketone [PEEK], polyphenylene sulfide [PPS]). Upon curing, thermosets form a highly cross-linked, three-dimensional molecular network that does not melt at high temperatures. Thermoplastics, however, are based on polymer chains that do not cross-link. As a result, thermoplastics will soften and melt at high temperatures, then harden again upon cooling.

Epoxies and polyesters have been the principal polymer matrix materials for several decades, but advanced thermoplastics such as PEEK and PPS are now receiving considerable attention for their excellent toughness and low moisture absorption properties, their simple processing cycles, and their higher-temperature capabilities. Aerospace grade epoxies are typically cured at about 177°C (350°F) and are generally not used at temperatures above 150°C (300°F), whereas advanced thermoplastics such as PPS, PI, and PEEK have melting temperatures in the range 315 to 370°C (600 to 700°F). At this time, it appears that polymer matrix materials for use up to 425°C (800°F) are feasible. For higher temperatures, metal, ceramic, or carbon matrix materials are required.

By using lightweight metals such as aluminum, titanium, and magnesium and their alloys and intermetallics such as titanium aluminide and nickel aluminide, operating temperatures can be extended to about 1250°C (2280°F). Other advantages of metal matrices are higher strength, stiffness, and ductility than polymers but at the expense of higher density. Ceramic matrix materials such as silicon carbide and silicon nitride can be used at temperatures up to 1650°C (3000°F). Ceramics have poor tensile strength and are notoriously brittle, however, and there is a need for much research before these materials can be routinely used. Finally, carbon fiber/carbon matrix composites can be used at temperatures approaching 2760°C (5000°F), but the cost of these materials is such that they are used only in a few critical aerospace applications. For further details on matrix materials and their properties, the reader is referred to any of several handbooks [8–13]. Matrix properties will be discussed again in chapter 3, where properties for typical matrix materials will be given.

The third constituent material of a composite, the filler material, is mixed in with the matrix material during fabrication. Fillers are not generally used to improve mechanical properties but, rather, are used to enhance some other aspect of composite behavior. For example, hollow glass microspheres are used to reduce weight, clay or mica particles are used to reduce cost, carbon black particles are used for protection against ultraviolet radiation, and alumina trihydrate is used for flame and smoke suppression [11]. Fillers truly add another dimension to the design flexibility we have in composites.

1.3 Structural Applications of Composites

Composite structural elements are now used in a variety of components for automotive, aerospace, marine, and architectural structures in addition to consumer products such as skis, golf clubs, and tennis rackets. Since much of the current composites technology evolved from aerospace applications, it is appropriate to begin this brief overview there.

Military aircraft designers were among the first to realize the tremendous potential of composites with high specific strength and high specific stiffness, since performance and maneuverability of those vehicles depend so heavily on weight. Composite construction also leads to smooth surfaces (no rivets or sharp transitions as in metallic construction), which reduce drag. Since boron and graphite fibers were first developed in the early 1960s, applications of advanced composites in military aircraft have accelerated quickly. Composite structural elements such as horizontal and vertical stabilizers, flaps, wing skins, and various control surfaces have been used in fighter aircraft such as the F-14, F-15, F-16, ..., F-22 (fig. 1.7). The steady growth in the use of composite structures in military fighter aircraft in recent years is shown graphically in figure 1.8. Not shown in

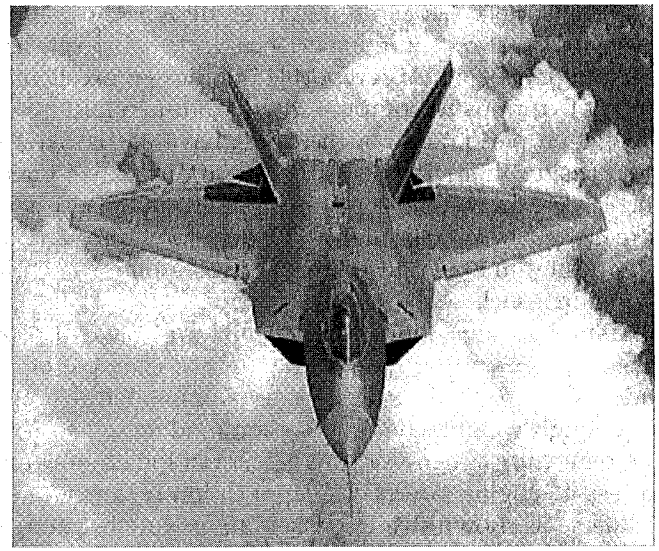

FIGURE 1.7
Lockheed Martin F-22 Raptor. (From Harris, C.E., Starnes, J.H., Jr., and Shuart, M.J. 2001. *An Assessment of the State-of-the-Art in the Design and Manufacturing of Large Composite Structures for Aerospace Vehicles*. NASA TM-2001-210844.)

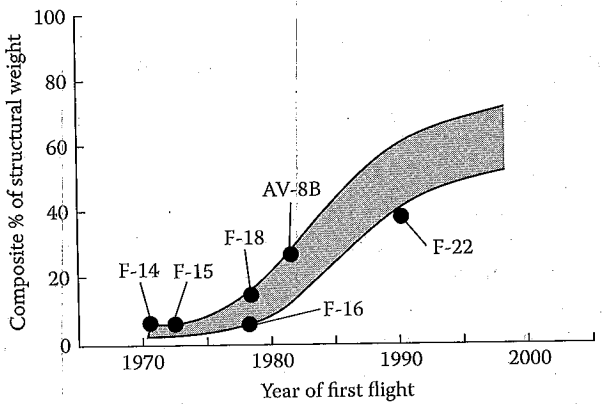

FIGURE 1.8
Composite structural applications in military fighter aircraft. (From Harris, C.E., Starnes, J.H., Jr., and Shuart, M.J. 2001. *An Assessment of the State-of-the-Art in the Design and Manufacturing of Large Composite Structures for Aerospace Vehicles*. NASA TM-2001-210844).

figure 1.8 are the data for the B-2 Stealth bomber, which has a primary structure consisting of essentially all composite materials [14].

Composites applications in commercial aircraft have been steadily increasing as material costs come down, as design and manufacturing technology evolves, and as the experience with composites in aircraft continues to build. A 1994 NASA report [15] indicated excellent in-service performance of composite components in commercial aircraft over a 15-year evaluation period, and such results have encouraged increased usage of composites in aircraft structures, including small business-type aircraft and large, commercial-transport aircraft. Initial use in these aircraft was restricted to smaller, lightly loaded secondary structures, but recently composites are being used increasingly in large, heavily loaded primary structures such as the wings and the fuselage. For example, the Cirrus SR-22 single-engine, four-passenger aircraft shown in figure 1.9 has a composite fuselage and wings. As an excellent example of innovative design made possible by composites, the use of composites in this airplane resulted in enough weight savings to accommodate the extra weight of an airframe parachute system for safe descent of the entire aircraft in the event of a loss of engine power. The application of composites in commercial airliners has shown steady, conservative growth, but based on the increased prices of fuels, demands by airlines for more efficient aircraft, and other recent trends, this growth promises to be rapid in the future. About 10% of the structural weight of the Boeing 777 (fig. 1.10) consists of composite materials, primarily graphite/epoxy [14]. However, based on the performance record of composites in the 757/767/777 series and

FIGURE 1.9
Cirrus SR-22 single engine, four passenger composite aircraft. (Courtesy of Cirrus Design Corporation.)

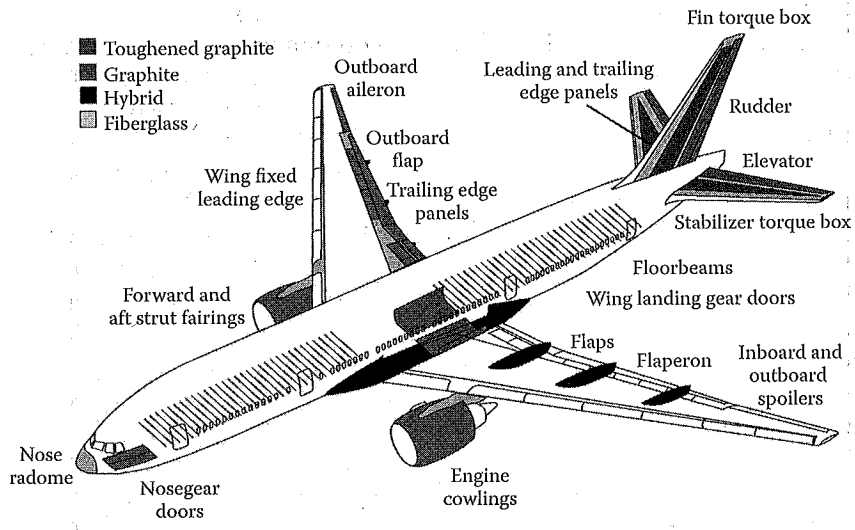

FIGURE 1.10
Applications of composites in the Boeing 777 airliner. (Courtesy of Boeing.)

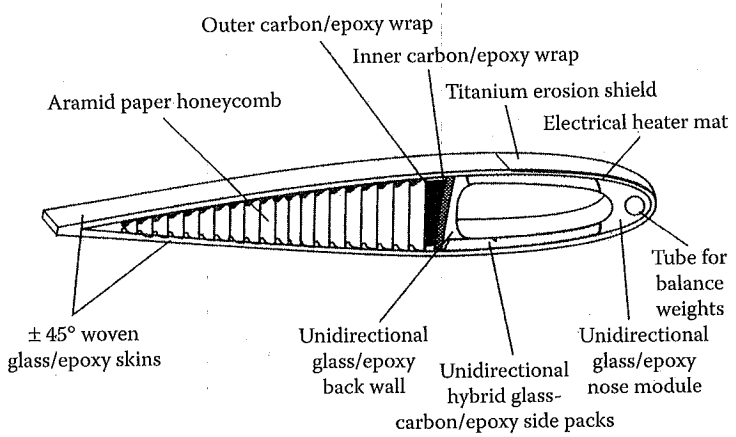

FIGURE 1.11
Composite construction of a helicopter rotor blade. (From McCrum, N.G., Buckley, C.P., and Bucknall, C.B. 1988. *Principles of Polymer Engineering* [Oxford University Press, New York]. Copyright 1988, Oxford University Press. Reprinted by permission.)

other airliners, the Boeing 787 will be the first commercial airliner with a composite fuselage and wings, and is expected to enter service in 2008. A similar new airliner, the Airbus A350, with composite wings and rear section fuselage, is expected to enter service in 2010.

The level of sophistication attained in aircraft composite construction is strikingly illustrated by the composite helicopter rotor blade in figure 1.11. The construction of such a component obviously requires a multistep fabrication procedure involving many materials, and some of these fabrication processes will be discussed in the next section.

Due to the tremendous cost per unit weight to place an object in space, the value of weight saved is even greater for spacecraft. Thus, composites are extremely attractive for spacecraft applications. The NASA Space Shuttle has a number of composite parts, including graphite/epoxy cargo bay doors and experimental graphite/epoxy solid rocket-booster motor cases. For large space structures such as the proposed space station, the key properties of the structural materials are high stiffness-to-weight ratio, low thermal expansion coefficient, and good vibration-damping characteristics. In all three of these areas composites offer significant advantages over conventional metallic materials.

Scaled Composite's SpaceShipOne (fig. 1.12), the first private manned spacecraft to achieve suborbital flight, is constructed primarily from composite materials, and promises to lead the way to commercial manned

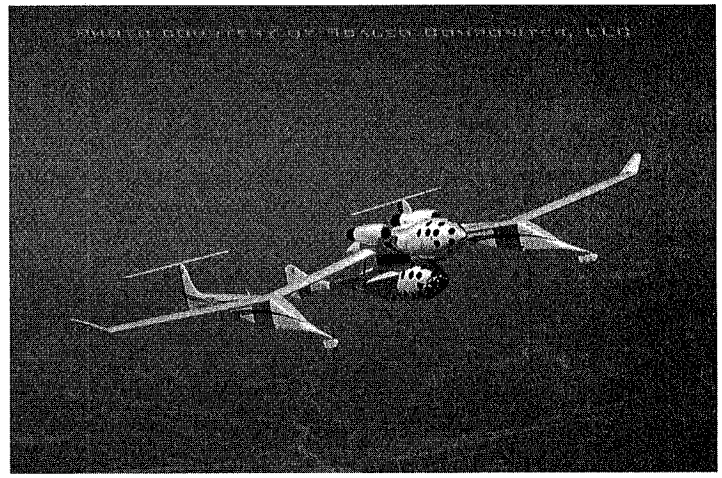

FIGURE 1.12
SpaceShipOne and its mother ship White Knight. (© 2004 Mojave Aerospace Ventures LLC, photograph by Scaled Composites. SpaceShipOne is a Paul G. Allen project.)

space travel. In other spacecraft components such as precision reflectors (fig. 1.13), special composite structures such as carbon fiber-reinforced isogrids are used for their superior dimensional stability characteristics. As shown later, some advanced fibers such as carbon have extremely low (and in some cases, negative) thermal expansion coefficients, which makes it possible to design composite structures having excellent dimensional stability.

Structural weight is also very important in automotive vehicles, and the use of composite automotive components continues to grow. Glass fiber–reinforced polymers continue to dominate the automotive composites market, but advanced composites with carbon fiber reinforcement are getting increased attention as the cost of carbon fibers continues to drop. In cargo trucks, the reduced weight of composite components translates into increased payloads, which can have a significant economic impact. For example, the composite concrete mixer drum shown in figure 1.14 weighs 2000 lb less than the conventional steel mixer drum that it replaced. According to the manufacturer, this means that an additional one-half cubic yard of concrete per load can be transported, which translates into an estimated productivity gain of $7500 per year.

Weight savings on specific components such as composite leaf springs can exceed 70% compared with steel springs (composite leaf springs have also proved to be more fatigue resistant). Experimental composite engine

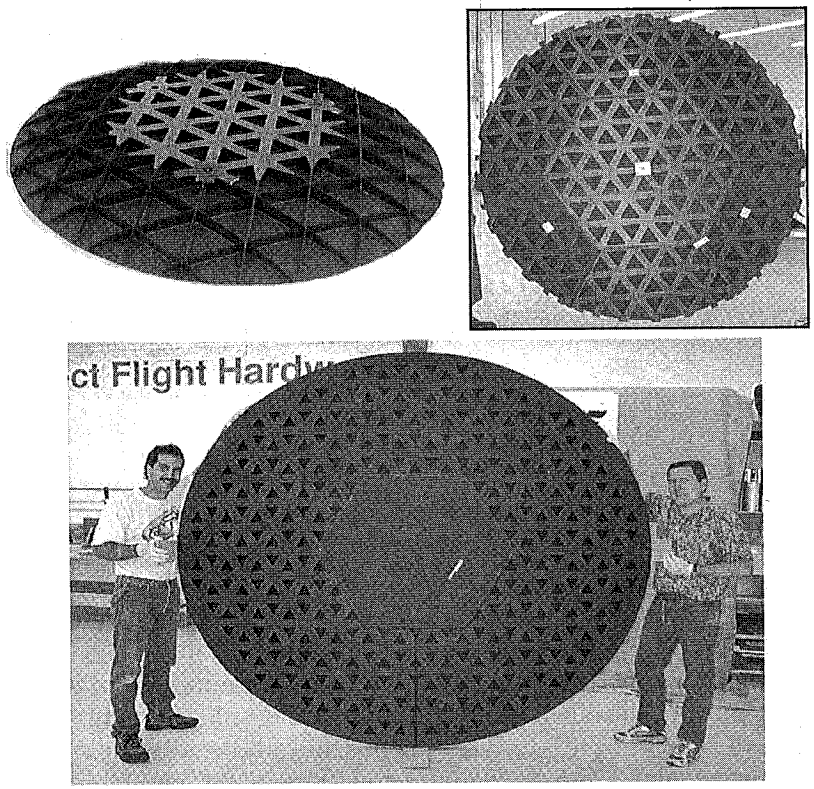

FIGURE 1.13
Composite isogrid spacecraft reflector. (Courtesy of Composite Optics, Inc.)

blocks have been fabricated from graphite-reinforced thermoplastics, but the ultimate goal is a ceramic composite engine that would not require water cooling. Chopped glass fiber–reinforced polymers have been used extensively in body panels (fig. 1.15) where stiffness and appearance are the principal design criteria. Composite primary structures such as Automotive Composites Consortium's composite "body-in-white" (fig. 1.16) are only experimental at this point, but they offer weight reduction, fewer parts, and smaller assembly and manufacturing costs. As with airliners, so far the applications of composites in automotive vehicles have been mainly in secondary structural elements and appearance parts, and the full potential of composite primary structures remains to be explored.

Other applications of structural composites are numerous, so only a few examples will be given here. I-beams, channel sections, and other structural elements (fig. 1.17) used in civil infrastructure may be made of fiber-reinforced plastic using the pultrusion process, which will be discussed

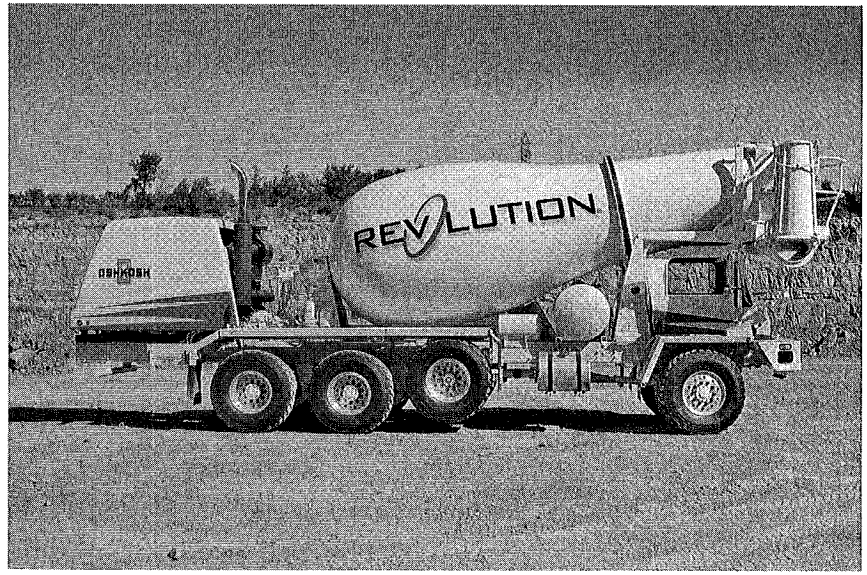

FIGURE 1.14
Composite mixer drum on concrete transporter truck weighs 2000 lb less than conventional steel mixer drum. (Courtesy of Oshkosh Truck Corporation.)

FIGURE 1.15
Ford Thunderbird with composite body panels. (Courtesy of Ford Motor Company, Research Staff.)

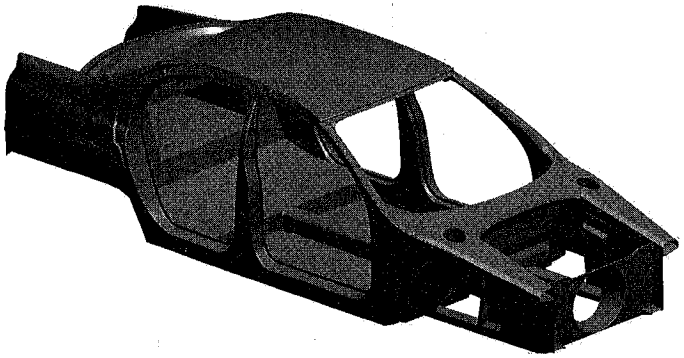

FIGURE 1.16
Automotive Composites Consortium's composite "body-in-white" concept. (Courtesy of Automotive Composites Consortium.)

in the next section. Corrosion resistance and electrical and thermal insulation are added advantages of composites over steel in such applications. Wind turbines (fig. 1.18) are getting increased attention as environmentally attractive, alternative energy sources, and their blades are typically made from composites due to their high strength-to-weight ratio, high stiffness-to-weight ratio, excellent vibration damping, and fatigue resistance. The bodies of large mass-transportation vehicles such as airport

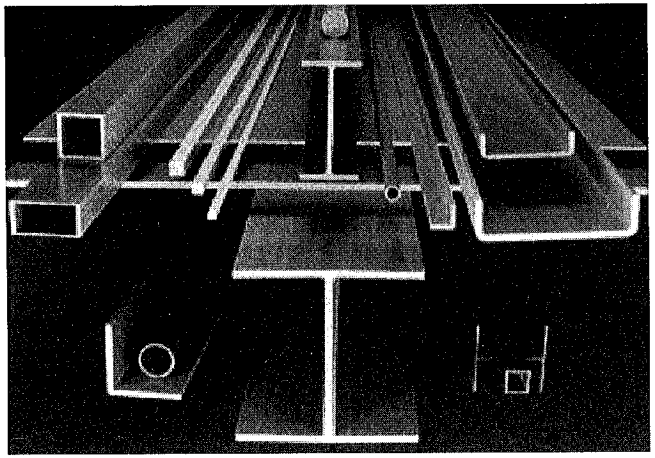

FIGURE 1.17
Pultruded fiberglass composite structural elements. (Courtesy of Strongwell Corporation.)

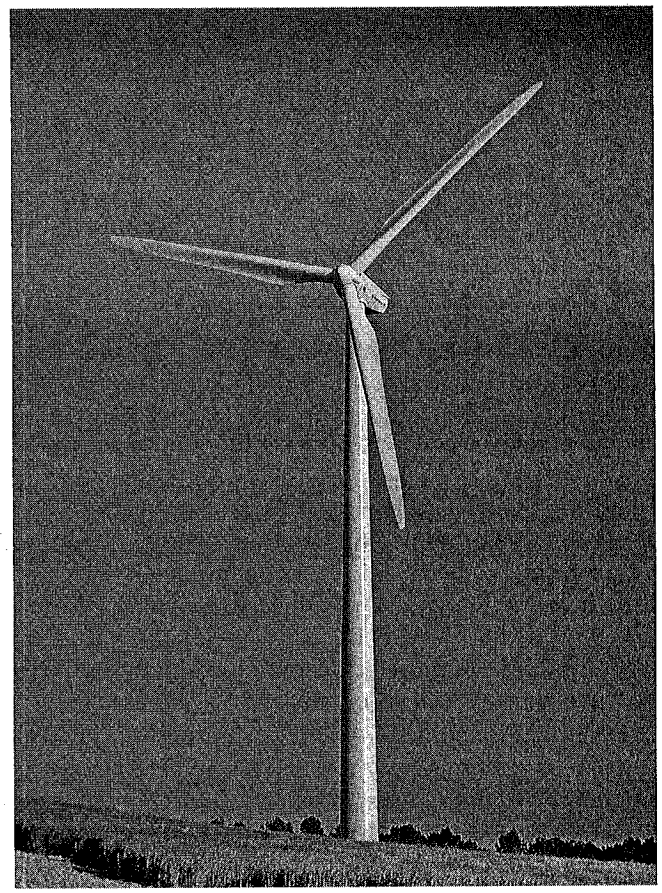

FIGURE 1.18
Composite wind turbine blades. (Courtesy of GE Energy.)

people movers (fig. 1.19) are often fabricated from composites for the same reasons that they are used in many other transportation vehicles, and because, as shown in the next section, high-volume, low-cost processes for fabricating such large structures are now believed to be relatively mature technologies. One of the fastest growing applications of composites in civil infrastructure is in prefabricated bridge decks for either new bridges or rehabilitation of older bridges. Fiber-reinforced polymer (FRP) composite bridge decks (fig. 1.20) have many advantages over conventional concrete and steel decks: FRP decks weigh much less, are more resistant to corrosion and freeze–thaw cycles, and are more easily and

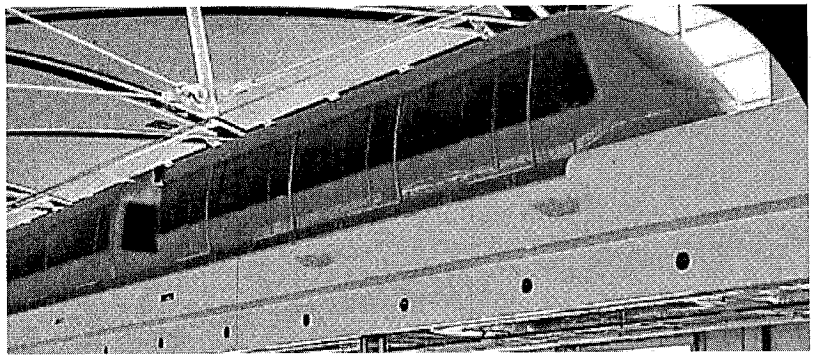

FIGURE 1.19
Airport people mover with composite body. (Courtesy of TPI Composites.)

quickly installed. A major related application is the now common practice of seismic retrofitting of conventional concrete–steel bridge columns by wrapping them with composite tapes in earthquake-prone areas. In these examples, as well as in many of the previous examples, cost is a major consideration limiting the more widespread use of composites. The fabrication process is the key to cost control, and the next section will describe the fabrication processes used to make the components described here.

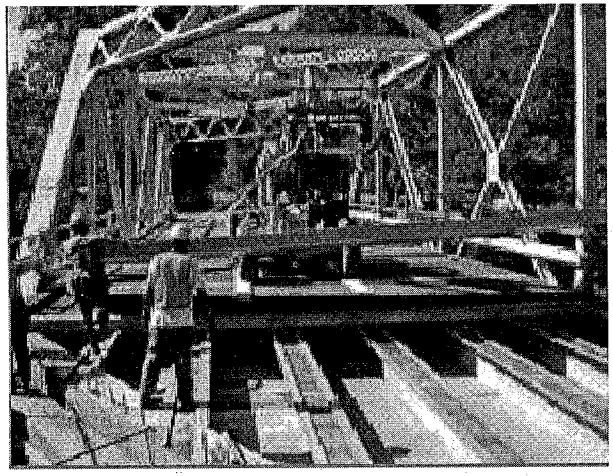

FIGURE 1.20
Installation of FRP composite deck for bridge rehabilitation. (Courtesy of Martin Marietta Composites.)

1.4 Fabrication Processes

Although this book is concerned primarily with the mechanics of composite materials, it is essential for the reader to know how these materials are made. This is because, with composites, we design and build not only the structure, but also the structural material itself. The selection of a fabrication process obviously depends on the constituent materials in the composite, with the matrix material being the key (i.e., the processes for polymer matrix, metal matrix, and ceramic matrix composites are generally quite different). In this summary of fabrication processes, only those used for polymer matrix composite fabrication will be discussed, and the reader is referred to other books for details on metal matrix and ceramic matrix composite fabrication [8–13,16].

A summary of fabrication processes used for polymer composites with various types of fiber reinforcement is given in table 1.2. The open mold process with hand lay-up of woven fiber mat or chopped strand mat (fig. 1.21) or spray-up of chopped fibers (fig. 1.22) is used for development work, prototype fabrication, and production of large components in relatively small quantities. A mold having the desired shape is first coated with a mold release, which prevents bonding of the resin matrix material to the mold. If a smooth surface on the part is desired (i.e., boat hulls or aircraft exterior parts), a gel coat is then applied to the mold, followed by a thermosetting polymer resin and the fibers. A roller may then be used for consolidation, followed by curing the polymer resin at the required temperature.

TABLE 1.2
Fabrication Processes for Polymer Matrix Composites

Process	Type of Reinforcement			
	Continuous	Chopped	Woven	Hybrid
Open mold				
Hand lay-up		X	X	
Spray-up		X		
Autoclave	X		X	
Compression molding	X	X	X	X
Filament winding	X			
Roll-wrapping	X		X	
Pultrusion	X		X	
Liquid composite molding	X	X	X	X
Reinforced reaction injection molding		X		
Resin infusion	X	X	X	X
Automated fiber placement	X		X	
Thermoplastic molding	X	X	X	X
Programmable powdered preform process		X		

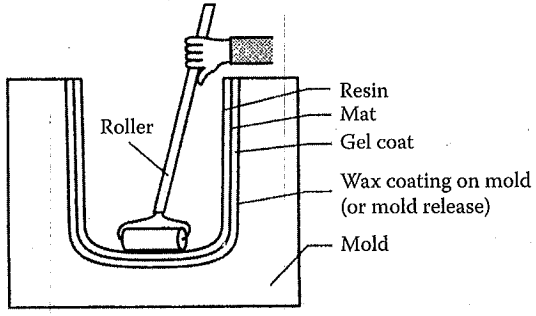

FIGURE 1.21
Open mold, hand lay-up composite fabrication.

A major breakthrough in composite manufacturing technology was the development of "prepreg tape," which is a tape consisting of fibers precoated with the polymer resin. This innovation means that the fabricator no longer has to worry about mixing the resin components in the right proportions and combining the resin with the fibers in the correct fashion. Most prepreg tape is made by the hot-melt process (fig. 1.23). If a thermosetting resin is used, the resin coating is partially cured, and the tape must be kept refrigerated to prevent full curing until final use. If a thermoplastic resin is used, the tape can be stored at room temperature until it is melted during final use. The fabrication of a laminated structure with prepreg tape involves simply "laying-up" the tape at the required orientation on a mold, stacking layers of tape in the required stacking sequence, and then curing the assembly under elevated temperature and pressure.

Autoclave molding (fig. 1.24) is the standard aerospace industry process for fabrication with prepreg tapes. The autoclave is simply a heated pressure

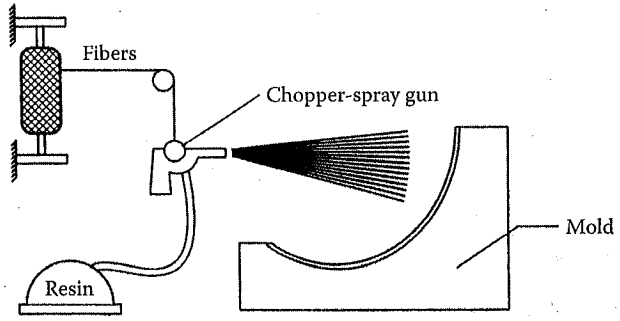

FIGURE 1.22
Open mold, spray-up composite fabrication.

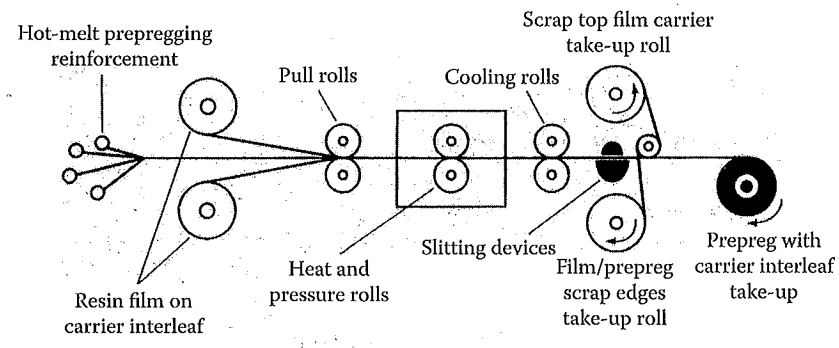

FIGURE 1.23
Hot-melt prepregging process. (Courtesy of Suppliers of Advanced Composite Materials Association [SACMA].)

vessel into which the mold (with lay-up) is placed and subjected to the required temperature and pressure for curing. The mold and lay-up are often covered with a release fabric, a bleeder cloth, and a vacuum bag. A vacuum line is then attached to the mold for evacuation of volatile gases during the cure process. Without the vacuum bagging, these gases would be trapped and could cause void contents of greater than 5% in the cured laminate. With the vacuum bag, void contents of the order of 0.1% are attainable. Autoclaves come in a wide range of sizes, from bench-top laboratory versions to the room-size units used to cure large aircraft structures. The autoclave-style press cure [17] is often used to cure small samples for research. In this case, a vacuum-bagged mold assembly (fig. 1.25) is inserted between the heated

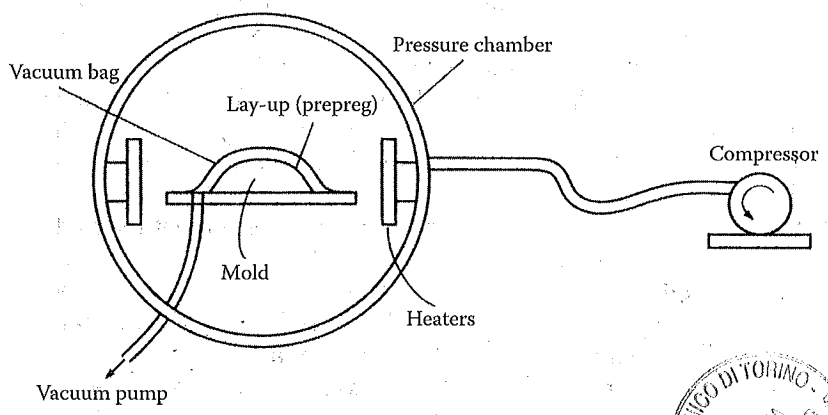

FIGURE 1.24
Autoclave molding.

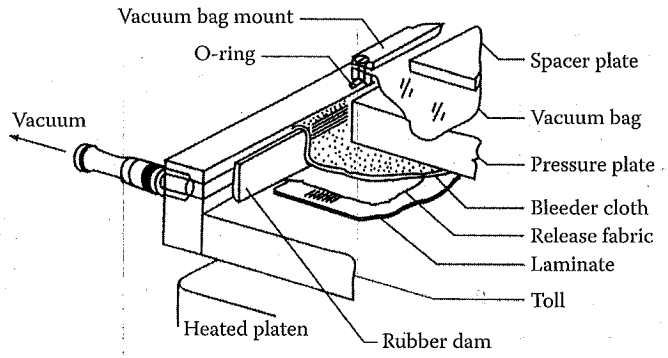

FIGURE 1.25
Lay-up sequence for autoclave-style press molding.

platens of a hydraulic press, and the press then generates the temperature and pressure required for curing. A vacuum press is a variation on this concept involving the use of a vacuum chamber surrounding the platen-mold assembly, and a sealed door on this chamber eliminates the need for a vacuum bag.

Sheet-molding compounds (SMCs) are an important innovation in composite manufacturing that are used extensively in the automobile industry. SMCs are similar to prepreg tape in that the fibers and the resin are "prepackaged" in a form that is more easily usable by fabricators. SMCs consist of a relatively thick, chopped fiber–reinforced resin sheet, whereas prepreg usually has continuous fibers in a thin tape. A machine for producing SMCs is shown schematically in figure 1.26. An alternative to SMCs are bulk-molding compounds (BMCs), which consist of the chopped fiber/resin mixture in bulk form. SMCs or BMCs may be molded by using the matched metal die process (fig. 1.27).

Filament winding (fig. 1.28), which involves winding resin-coated fibers onto a rotating mandrel, may be used to produce any composite structure having the form of a body of revolution. Fiber orientation is controlled by the traverse speed of the fiber winding head and the rotational speed of the mandrel. Another advantage of this process is that by controlling the winding tension on the fibers, they can be packed together very tightly to produce high-fiber-volume fractions. Upon completion of the winding process, the composite structure may be cured by placing the mandrel in an oven or by passing hot fluid through the mandrel itself.

Filament winding is widely used to produce such structures as rocket motor cases, pressure vessels, power transmission shafts, piping, and tubing. Prepreg tape is often produced by filament winding and removing

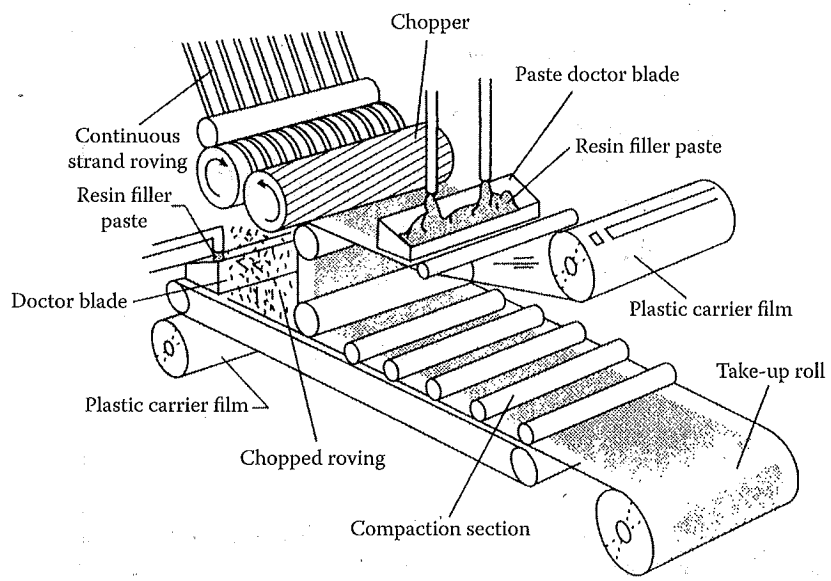

FIGURE 1.26
Machine for producing SMCs. (From Reinhart, T.J. et al. eds. 1987. *Engineered Materials Handbook*, vol. 1, *Composites* [ASM International, Materials Park, OH]. Reprinted by permission of ASM International.)

the tape from the mandrel before curing. Imaginative variations on the filament winding process have produced a variety of structures such as leaf springs for automotive vehicles. A composite leaf spring may be fabricated by winding on an ellipsoidal mandrel, then cutting the cured shell into the required pieces. Experimental programs are underway to produce large, complex structures such as aircraft fuselages and automobile body

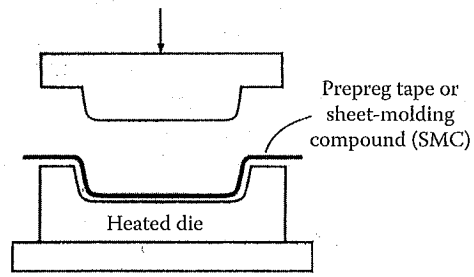

FIGURE 1.27
Compression molding with matched metal dies.

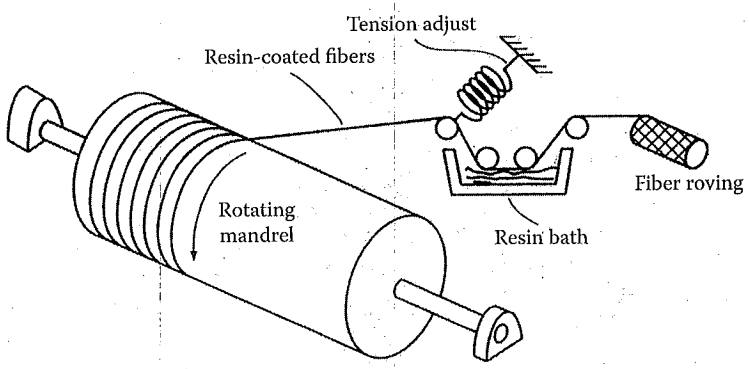

FIGURE 1.28
Filament winding process.

structures by filament winding. Filament winding machines for such structures will require the liberal use of computer control and robotics.

The roll wrapping (or tube rolling) process also involves the placement of resin-impregnated fibers on a cylindrical mandrel to produce a composite tube or other body of revolution. However, in the case of roll wrapping, sheets of composite prepreg tape are wrapped around the mandrel by rolling the mandrel over the prepreg, which lies flat on a table. In this manner, prepreg tape is wrapped around the mandrel at a rate of one layer per revolution, and the mandrel is indexed after each revolution so that the abutting joints of prepreg tape are offset by some amount, thus avoiding an undesirable region of weakness that would be generated if all the abutting joints line up along a radial line. Once the wrapping process is completed, the mandrel is externally pressurized and heated at the required cure pressure and temperature. One advantage of roll wrapping over filament winding is that the fibers can be oriented in the true circumferential direction for maximum hoop strength, whereas in filament winding, some amount of deviation from circumferential fiber orientation will be introduced as the winding head traverses along the rotating mandrel. Either unidirectional fiber or woven fabric–reinforced prepreg can be used in roll wrapping, whereas filament winding is typically restricted to unidirectional fiber tows. Roll wrapping is often used to produce fishing rods, golf club shafts, hockey sticks, and tubing for bicycle frames.

Many of the processes described above are fairly time consuming. Processes with faster production cycles are needed for high-volume applications such as automotive parts. For example, reinforced reaction injection molding (RRIM) is a very fast process that is widely used to produce such components as automobile body panels. The RRIM process (fig. 1.29) involves the injection of a chopped fiber/resin mixture into a mold under

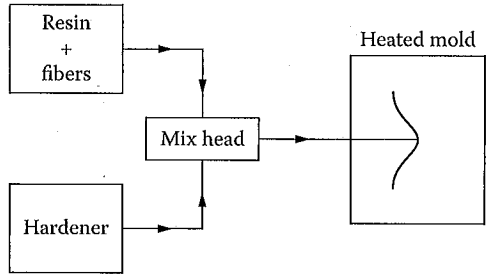

FIGURE 1.29
RRIM process.

high pressure and then curing it at the required temperature. "Pultrusion" (fig. 1.30) is the process of pulling a continuous fiber/resin mixture through a heated die to form structural elements such as I-beams and channel sections (fig. 1.17). This process is relatively fast but is restricted to structures whose shapes do not change along the length. In the thermoplastic molding process (fig. 1.31), a blank (an uncured laminate consisting of thermoplastic prepreg tape layers) is passed through an infrared oven where it is heated to near the melting point of the thermoplastic resin. Thermoplastic yarn or woven textiles consisting of commingled reinforcing fibers and thermoplastic matrix fibers (fig. 1.32) are also used. The heated blank is then quickly placed in a matched metal die mold for final forming. In another form of thermoplastic molding, solid cylindrical pellets containing either long or short chopped fibers in a thermoplastic resin are melted and molded by using a screw injection machine, or by compression molding. Resin transfer molding (RTM) and structural reaction injection molding (SRIM) are attracting considerable attention because of their relatively fast production cycles and the near-net-shape of resulting parts. In both the RTM process (fig. 1.33) and the SRIM process, a "preform"

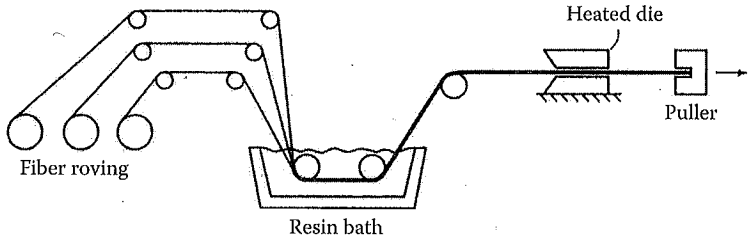

FIGURE 1.30
Pultrusion process.

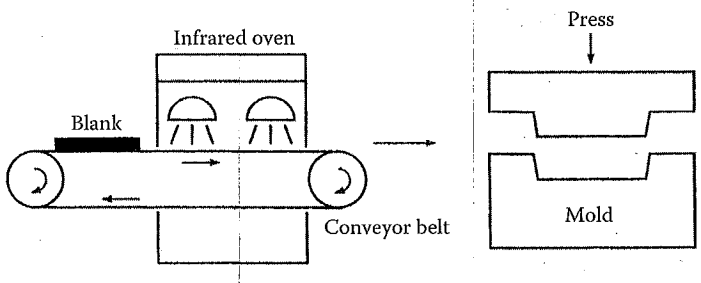

FIGURE 1.31
Thermoplastic molding process.

consisting of fibers and possibly a foam core is first produced in the general shape of the finished part. The preform is then placed in a closed metal mold and the liquid resin is injected under pressure. The major difference between the two processes is that with RTM, the resin and hardener are premixed before injection into the mold, whereas with SRIM, the resin and hardener are mixed by impingement as they are injected into the mold. Three-dimensionally shaped parts with foam cores can be produced with both RTM and SRIM, but SRIM tends to be faster than RTM.

In the vacuum-assisted RTM (VARTM) process, a vacuum pump is connected to the closed mold to pull the resin through the fiber preform. The SCRIMP™ (Seeman composites resin infusion molding process) shown in figure 1.34 is an open mold/vacuum bag version of the VARTM

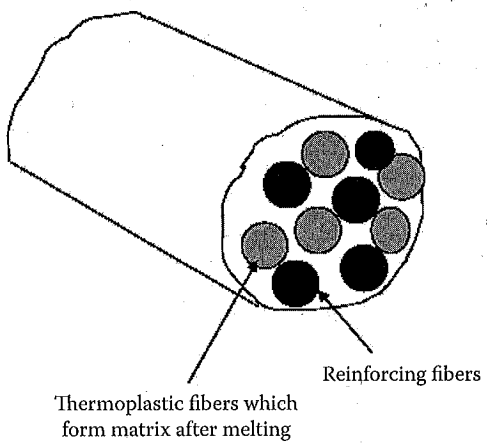

FIGURE 1.32
Commingled reinforcing fibers and thermoplastic matrix fibers in a thermoplastic yarn.

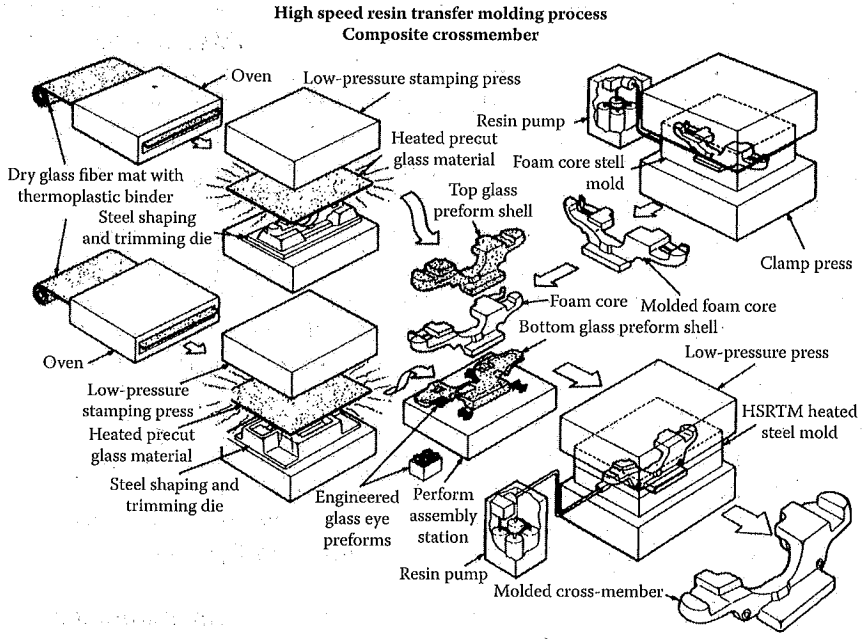

FIGURE 1.33
RTM process. (Courtesy of Ford Motor Company, Research Staff.)

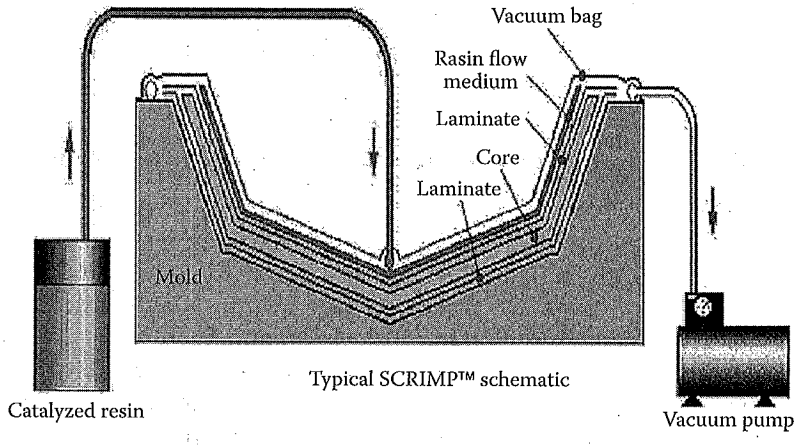

FIGURE 1.34
Schematic of SCRIMP™ (Seeman composites resin infusion molding process). (Courtesy of TPI Composites.)

process; it is effective for fabricating very large composite structures. The resin film infusion (RFI) process is similar to the SCRIMP™ process except that a solid resin film is used instead of a liquid resin. In RFI, the lay-up consists of the fiber preform and a solid resin film covered with a vacuum bag in an open mold, followed by heating and melting of the resin film, which infuses the fiber preform. Finally, the composite part is cured and released from the mold. The automated fiber placement process involves robotic placement of thermoset or thermoplastic prepreg tapes on a mold and is widely used in the aerospace industry. In processing methods that involve fiber preforms, one of the most costly and time-consuming steps is the fabrication of the fiber preform itself. An innovative breakthrough in preform fabrication involves the use of robotic fiber placement in the so-called P4 (programmable powder preform process). In the P4 process, continuous fibers are chopped and sprayed onto a mold screen by a programmable robot, along with a small amount of resin binder to hold the fibers in place. A vacuum also helps to hold the fibers in place on the screen. The completed fiber preform is removed from the screen and placed in a mold where it is infiltrated with resin that is cured to form the composite part.

In conclusion, many innovative processes exist for manufacturing polymer composites. Much of the success that composite materials have had in the past several decades is due to innovative fabrication technology, and the future success of composites will surely depend on further advances in this area. Computer-aided-manufacturing technology and robotics are expected to play important roles in the continuing drive to reduce cost and to improve the quality of composite structures.

1.5 Elements of Mechanical Behavior of Composites

This book is concerned with the analysis of both the micromechanical and the macromechanical behavior of fiber-reinforced composite materials. As shown schematically in figure 1.35, micromechanics is concerned with the mechanical behavior of constituent materials (in this case, fiber and matrix materials), the interaction of these constituents, and the resulting behavior of the basic composite (in this case, a single lamina in a laminate). Macromechanics is concerned with the gross mechanical behavior of composite materials and structures (in this case, lamina, laminate, and structure), without regard for the constituent materials or their interactions. As we will see in chapter 2, this macromechanical behavior may be characterized by averaged stresses and strains and averaged, or "effective," mechanical properties in an equivalent homogeneous material. As shown in chapter 3

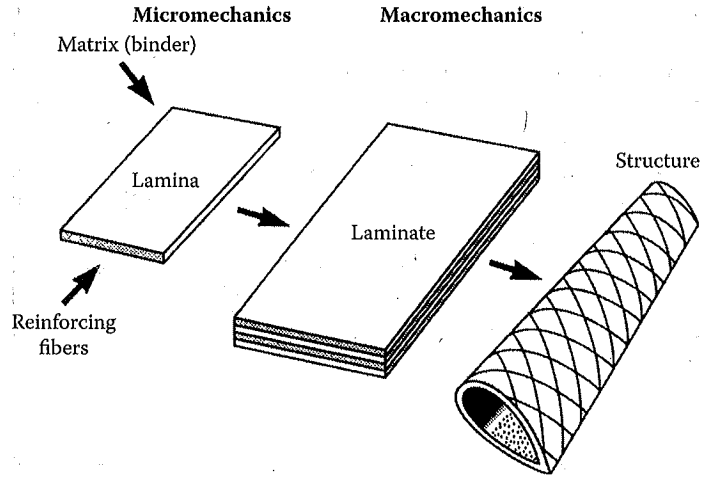

FIGURE 1.35
Micromechanics and macromechanics of composites.

to chapter 6, the focus in micromechanics is on the relationships between the effective composite properties and the effective constituent properties. Subsequent chapters deal with macromechanical behavior of laminates and structures.

When dealing with composite materials, we find very quickly that we can no longer draw upon the "intuition" about material behavior that we developed from years of experience with conventional metallic structural materials, and that we must learn to "think composites." Most metallic structural materials are homogeneous (properties do not vary from point to point in the material) and isotropic (properties do not depend on orientation), whereas most composites are heterogeneous and anisotropic. That is, the properties in a composite change as we move from matrix to fiber and as we change the direction along which they are measured. For example, in a "unidirectional" composite, having reinforcement in only one direction, the strength and stiffness are much greater along the reinforcement direction than in the transverse direction.

The relationships between forces and deformations (or between stresses and strains) are much more complicated in anisotropic composites than in conventional isotropic materials, and this can lead to unexpected behavior. For example, in an isotropic material, a normal stress induces only normal strains (extensions and/or contractions), and a shear stress induces only shear strains (distortions). In an anisotropic composite, however, a normal stress may induce both normal strains and

shear strains, and a shear stress may induce both shear strains and normal strains. A temperature change in an isotropic material causes expansion or contraction that is uniform in all directions, whereas a temperature change in an anisotropic material may cause nonuniform expansion or contraction plus distortion. These so-called "coupling" effects have important implications not only for the analytical mechanics of composites, but for the experimental characterization of composite behavior as well.

It is hoped that these general observations regarding composite materials will provide motivation for further study in subsequent chapters, where the analytical and experimental characterization of mechanical behavior of composites is discussed in more detail.

1.6 Review of Basic Mechanics of Materials Equations

The basic equations of the mechanics of materials are used throughout this book, and this section briefly reviews and reinforces those equations, with examples of application to composite systems. As shown in many textbooks on mechanics of solids [18,19], when the loading is static or quasistatic in nature, three basic categories of equations are typically used, separately or in combination, to solve problems in elementary mechanics of materials. They are:

- Equations of static equilibrium based on Newton's Second Law
- Force–deformation or stress–strain relationships for the materials
- Geometric compatibility equations or assumed relationships regarding the geometry of deformation

In addition, using accurate free-body diagrams is essential to setting up the correct equations of static equilibrium. The equations of mechanics of materials are often algebraic, but in some cases involving differential equations, a fourth category of equations, usually referred to as boundary conditions, is also needed. For example, the well-known beam-deflection equations are second-order ordinary linear differential equations whose solution requires two boundary conditions. In problems involving dynamic loading, equations of motion are used instead of static equilibrium equations, and the equations of motion may be either ordinary or partial differential equations, depending on whether the mass is assumed to be discretely or continuously distributed, respectively. Most of the cases

considered in this book will involve static or quasistatic loading, and dynamic loading is discussed mainly in chapter 8. Finally, it is important to recognize that, for statically determinant systems, the three categories of equations described above can be solved independently, but for statically indeterminate systems, they must be solved simultaneously.

The remainder of this section consists of examples demonstrating the application of the basic equations of mechanics of materials to the analysis of composite systems. These preliminary examples involve only simple composite systems having isotropic constituents, and the force–deformation and stress–strain relationships of isotropic materials should be familiar from previous studies of elementary mechanics of materials. However, it is important to realize that many composites and their constituents are anisotropic, and the corresponding force–deformation and stress–strain relationships of anisotropic materials are complex compared with those of isotropic materials. The study of anisotropic materials will begin in chapter 2.

EXAMPLE 1.1

We wish to find the stresses and deformations in the axially loaded composite bar system in figure 1.36a. The composite bar consists of two bars made of different isotropic materials A and B having different diameters and which are securely bonded together in a series arrangement and loaded by an axial load P. The bar of material A has length L_A, cross-sectional area A_A, and modulus of

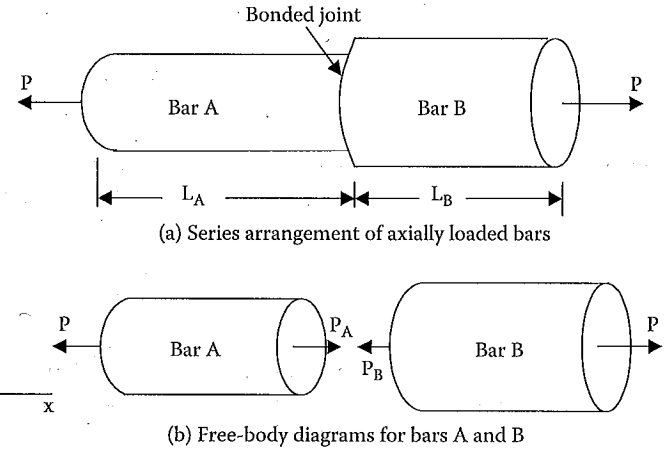

FIGURE 1.36
Composite bar system for example 1.1.

elasticity E_A, while the bar of material B has length L_B, cross-sectional area A_B, and modulus of elasticity E_B. Free-body diagrams of the two bars are shown in figure 1.36(b).

Solution. *For static equilibrium of bar A, which has internal force P_A,*

$$\sum F_x = P_A - P = 0 \tag{1.1}$$

Similarly, for bar B, which has internal force P_B,

$$\sum F_x = P - P_B = 0 \tag{1.2}$$

so that $P = P_A = P_B$ and the load is the same for each bar in the series arrangement.

The axial stresses in the two bars are therefore

$$\sigma_A = \frac{P_A}{A_A} \quad \text{and} \quad \sigma_B = \frac{P_B}{A_B} \tag{1.3}$$

The axial elongations of the bars are given by the familiar force–deformation equations

$$\delta_A = \frac{P_A L_A}{A_A E_A} \quad \text{and} \quad \delta_B = \frac{P_B L_B}{A_B E_B} \tag{1.4}$$

Since the bars are assumed to be securely joined together in a series arrangement, the total axial elongation is given by the geometric compatibility equation,

$$\delta_{total} = \delta_A + \delta_B \tag{1.5}$$

So for the series arrangement, the forces are the same in each member, and the total deformation is the sum of the deformations in the members. This is also an example of a statically determinate system, since the forces in the members can be determined from the static equilibrium equations alone. For such a system, the force–deformation equations and the geometric compatibility equation are not needed to find the forces in the members. The next example will be a statically indeterminate composite

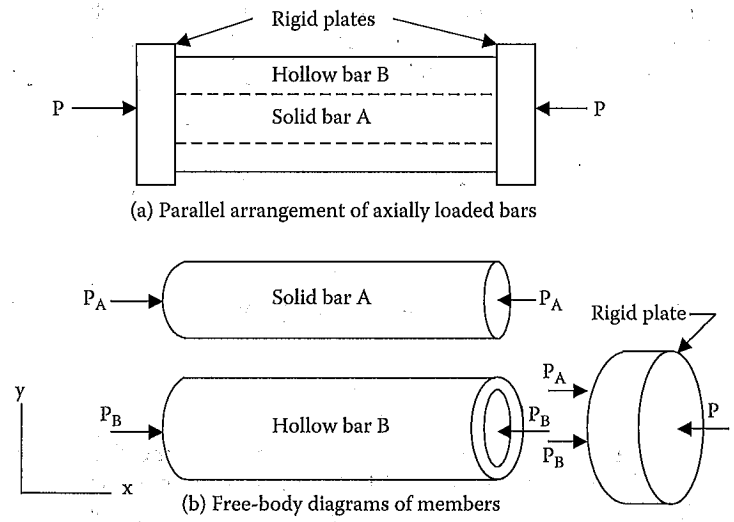

FIGURE 1.37
Composite bar system for example 1.2.

system, where the three basic types of equations must be solved simultaneously in order to find the forces in the members.

EXAMPLE 1.2
Now we wish to find the stresses and deformations in the composite system of figure 1.37(a), where a solid isotropic bar A is securely bonded inside a hollow isotropic bar B of the same length and both bars are axially loaded by a load P that is transmitted through rigid plates. The free-body diagrams for the bars and one of the rigid plates are shown in figure 1.37(b).

Solution. Static equilibrium of the rigid plate requires that the applied force P must be related to the internal forces in the members, P_A and P_B, by the equation

$$\sum F_x = P_A + P_B - P = 0 \quad \text{or} \quad P = P_A + P_B \tag{1.6}$$

This is the only nontrivial static equilibrium equation for this system, but the equation contains two unknown forces, P_A and P_B. Thus, unlike example 1.1, the forces in the members cannot be determined from the static equilibrium equations alone, and the system is said to be statically indeterminate. A second

equation is needed to solve for the two unknown forces, and that equation may be generated by combining the force–deformation relationships and the geometric compatibility condition. As with example 1.1, the force–deformation relationships for the bars are

$$\delta_A = \frac{P_A L_A}{A_A E_A} \quad \text{and} \quad \delta_B = \frac{P_B L_B}{A_B E_B} \tag{1.7}$$

Since the bars are assumed to be securely bonded together, the geometric compatibility condition for the parallel arrangement is

$$\delta_A = \delta_B \tag{1.8}$$

So for the parallel arrangement, the deformations in the members are equal and the total applied force is equal to the sum of the member forces. By combining the force–deformation and geometric compatibility equations, we obtain a second equation in the two unknown forces P_A and P_B that can be solved simultaneously with the static equilibrium equation. Once the forces P_A and P_B are found, the stresses and deformations in the members can be found.

EXAMPLE 1.3

In the composite system shown in figure 1.38(a), a rigid L-shaped bar is hinged at point O and is also supported by a wood post and a steel cable. Before the load P is applied, the system is unstressed, and we wish to find the stresses and deformations in the steel cable and the wood post after the load P is applied.

Solution. For a two-dimensional problem such as this, three static equilibrium equations are available, but from the free-body diagram of the L-shaped bar in figure 1.38(b), it is seen that there are four unknown reaction forces: the force in the steel cable, F_s, the hinge forces O_x and O_y, and the force in the wood post, F_w. The hinge forces are not of interest here, and can be eliminated from the problem by writing the equation for static equilibrium of moments about an axis through the hinge point O, as

$$\sum M_O = Pc - F_w b + F_s a = 0 \tag{1.9}$$

We now have one equation in two unknowns, F_w and F_s, and although there are two remaining available static equations, those equations would involve the hinge forces O_x and O_y, so nothing can be gained by considering them. Thus, the problem is statically indeterminate, and we must develop the geometric compatibility and force–deformation equations and solve all the equations simultaneously. The geometry of deformation

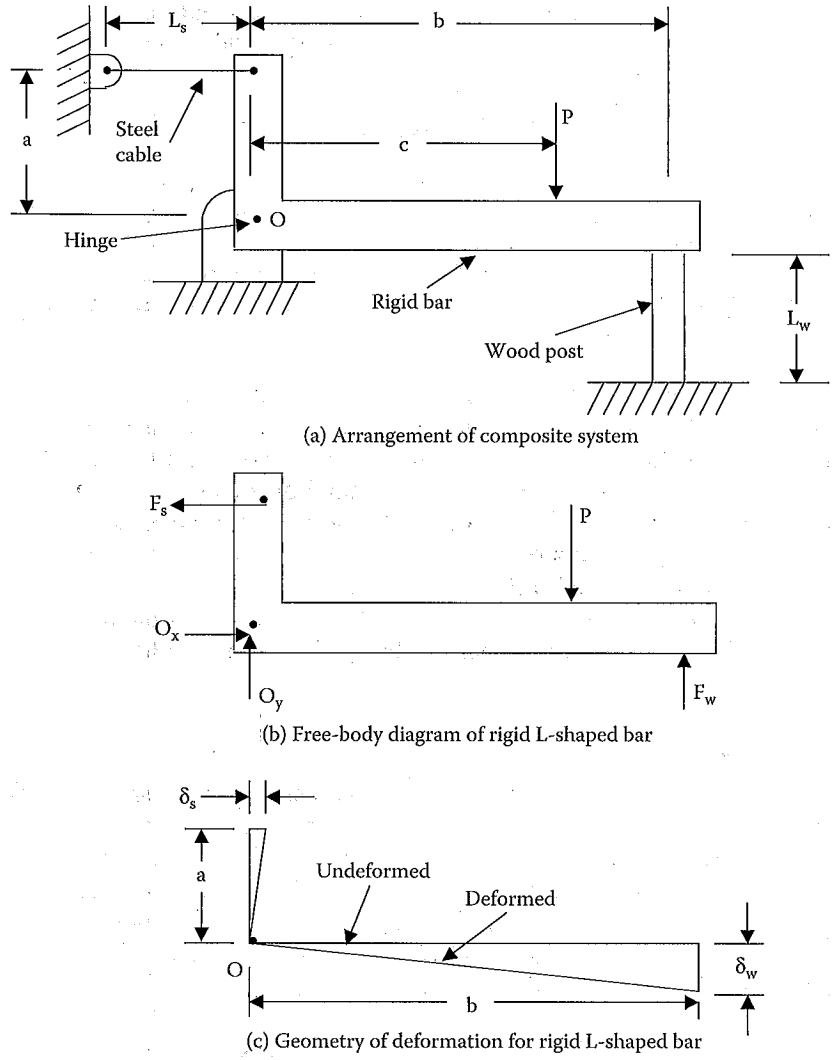

FIGURE 1.38
Composite system for example 1.3.

of the rigid L-shaped bar that rotates about the hinge point O is shown in figure 1.38(c). From this drawing, it is clear that the geometric compatibility equation is

$$\frac{\delta_w}{b} = \frac{\delta_s}{a} \tag{1.10}$$

where δ_w and δ_s are the deformations in the wood post and the steel cable, respectively. The corresponding force–deformation equations are

$$\delta_w = \frac{F_w L_w}{A_w E_w} \quad \text{and} \quad \delta_s = \frac{F_s L_s}{A_s E_s} \tag{1.11}$$

where A_w and A_s are the cross-sectional areas and E_w and E_s the elastic moduli of the wood post and the steel cable, respectively. Now the equilibrium, compatibility, and force–deformation equations can be solved simultaneously for the forces F_w and F_s; the forces and areas can then be used to determine the stresses.

Thus, the general procedure for analyzing statically indeterminate structures is to solve the static equilibrium equations, the force–deformation equations, and the geometric compatibility equations simultaneously for the forces in the members, then use the member forces to find the corresponding stresses and deformations. Although these same basic principles are used throughout this book, we find that it is often more convenient and practical to work with the stresses rather than the forces, the strains rather than the deformations, and the stress–strain relationships rather than the force–deformation relationships. Example 1.4 illustrates these concepts.

EXAMPLE 1.4

The composite ring assembly in figure 1.39 (a) consists of a thin steel inner ring of mean radius r_s, wall thickness t_s, modulus of elasticity E_s, and coefficient of thermal expansion α_s, which just fits inside an aluminum outer ring of mean radius r_a, wall thickness t_a, modulus of elasticity E_a, and coefficient of thermal expansion α_a, so that both rings are initially unstressed at room temperature. We wish to determine the stresses in each ring after the assembly has been cooled by an amount $\Delta T < 0$, where ΔT is the temperature drop.

Solution. From material property tables, we find that $\alpha_a \gg \alpha_s$, so that when the assembly is cooled, the aluminum ring tries to contract more than the steel ring. As a result of this differential contraction, a radial pressure, p, develops at the aluminum–steel interface, as shown in the free-body diagrams in figure 1.39(b). The effect of the interface pressure p is to put the inner steel ring in compression and the outer aluminum ring in tension. From the static equilibrium analysis of thin-walled cylinders or rings, which is found in any mechanics of materials book, the tangential (hoop) stresses in the two rings are

$$\sigma_a = \frac{pr_a}{t_a} \quad \text{and} \quad \sigma_s = -\frac{pr_s}{t_s} \tag{1.12}$$

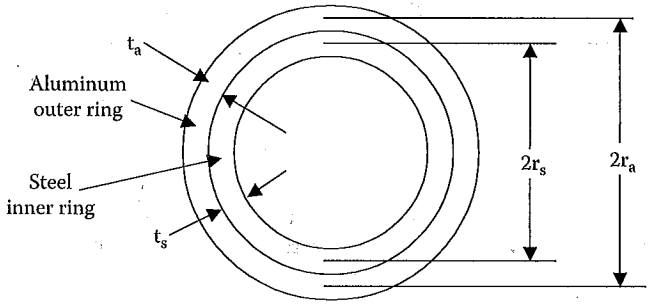

(a) Composite ring assembly

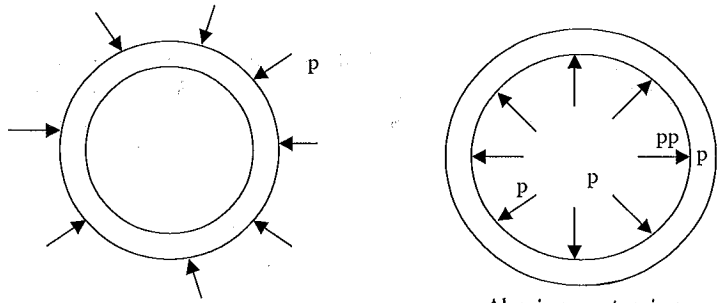

(b) Free-body diagrams of rings after cooling and differential contraction

FIGURE 1.39
Composite ring system for example 1.4.

However, it is clear from the free-body diagrams in figure 1.39(b) that the pressure p and the corresponding stresses above cannot be found from the static equilibrium equations alone. Thus, the system must be statically indeterminate, and we must develop additional equations based on geometric compatibility and stress–strain relationships.

From mechanics of materials, the tangential (hoop) strains in the rings must be

$$\varepsilon_a = \frac{\Delta r_a}{r_a} \quad \text{and} \quad \varepsilon_s = \frac{\Delta r_s}{r_s} \tag{1.13}$$

where Δr_a and Δr_s are the radial displacements in the aluminum and steel rings, respectively. Since the two rings are securely bonded together, geometric compatibility requires that $\Delta r_a = \Delta r_s$, so that

$$\varepsilon_a = \frac{r_s}{r_a}\varepsilon_s \tag{1.14}$$

The tangential stress–strain relationships for the two materials including thermal effects are

$$\varepsilon_a = \frac{\sigma_a}{E_a} + \alpha_a \Delta T \quad \text{and} \quad \varepsilon_s = \frac{\sigma_s}{E_s} + \alpha_s \Delta T \tag{1.15}$$

By combining the above equations, we can reduce the problem to one equation in one unknown, the interfacial pressure p, as shown below.

$$\frac{pr_a}{t_a E_a} + \alpha_a \Delta T = \frac{r_s}{r_a}\left(-\frac{pr_s}{t_s E_s} + \alpha_s \Delta T\right) \tag{1.16}$$

By substituting the known geometrical and material properties along with the temperature change, we can solve this equation for p. Once p is determined, the corresponding stresses in the rings can be easily calculated.

1.7 Problems

1. For a cylindrical particle, derive the relationship between the ratio of surface area-to-volume, A/V, and the particle aspect ratio, l/d, and verify the shape of the curve shown in figure 1.3.
2. Explain qualitatively why sandwich structures (fig. 1.5) have such high flexural stiffness-to-weight ratios. Describe the key parameters affecting the flexural stiffness-to-weight ratio of a sandwich panel.
3. Describe a possible sequence of fabrication processes that might be used to manufacture the helicopter rotor blade in figure 1.11. Note that several different materials and fiber lay-ups are used.
4. Which of the reinforcing fibers listed in table 1.1 would be best for use in an orbiting space satellite antenna structure that is subjected to relatively low stresses but has very precise dimensional stability requirements? The answer should be based only on the properties given in table 1.1.
5. A thin-walled filament wound composite pressure vessel has fibers wound at a helical angle θ, as shown in figure 1.40. Ignore the resin matrix material and assume that the fibers carry all of the load. Also assume that all fibers are uniformly stressed in tension. This gross oversimplification is the basis of the so-called "netting analysis," which is actually more appropriate for stress analysis of all-fiber textile fabrics. Using this simplified analysis, show that the angle θ must be 54.74° in order to support both the hoop (tangential) and axial stresses that are generated in a thin-walled pressure vessel. (See any mechanics of materials book for the stress analysis of a thin-walled pressure vessel.)

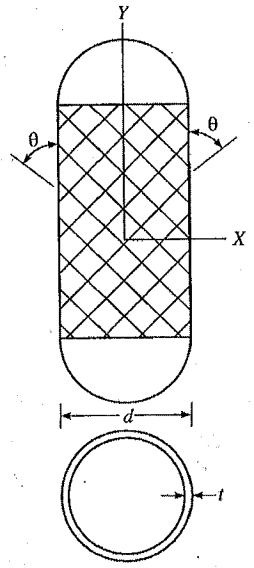

FIGURE 1.40
Filament wound composite pressure vessel for problem 5.

6. A filament wound E-glass/epoxy pressure vessel has a diameter of 50 in (127 cm), a wall thickness of 0.25 in (6.35 mm), and a helical wrap angle θ = 54.74°. Using a netting analysis and a safety factor of 2, estimate the allowable internal pressure in the vessel. Compare with the allowable internal pressure in a 6061-T6 aluminum alloy pressure vessel having the same dimensions. For the aluminum vessel, assume that the tensile yield stress is 40,000 psi (276 MPa) and use the Maximum Shear Stress yield criterion. Although the netting analysis is greatly oversimplified, these approximate results should demonstrate the significant advantages of fiber composite construction over conventional metallic construction.
7. The 2000 mm long composite bar shown in figure 1.41 consists of an aluminum bar having a modulus of elasticity $E_{Al} = 70$ GPa and length $L_{Al} = 500$ mm, which is securely fastened to a steel bar having modulus of elasticity $E_{St} = 210$ GPa and length $L_{St} = 1500$ mm. After

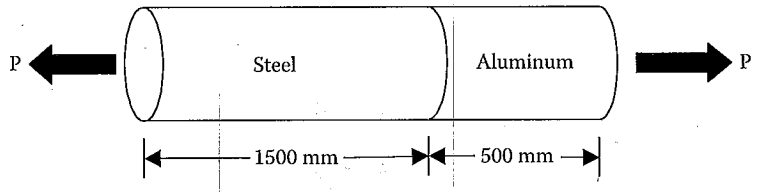

FIGURE 1.41
Composite bar system for problem 7.

the force P is applied, a tensile normal strain of $\varepsilon_{AL} = 1000 \times 10^{-6}$ is measured in the aluminum bar. Find the tensile normal stress in each bar and the total elongation of the composite bar.

8. A support cable in a structure must be 5 m long and must withstand a tensile load of 5 kN with a safety factor of 2.0 against tensile failure. Assuming a solid cylindrical cross-section for the cable as an approximation, (a) determine and compare the weights of cables made of 4340 steel and AS-4 carbon fibers that meet the above requirements, and (b) for an AS-4 carbon fiber cable having the same weight, length, and safety factor as the 4340 steel cable from part (a). How much tensile load will the carbon fiber cable be able to withstand?
9. A flywheel for energy storage is modeled as a rotating thin-walled cylindrical ring ($t << r$) as shown in figure 1.42. Find the equation for the tensile stress in the ring as a function of the mean radius, r, the rotational speed, ω, and the mass density, ρ, of the ring, then compare the maximum peripheral speed (tangential velocity) and

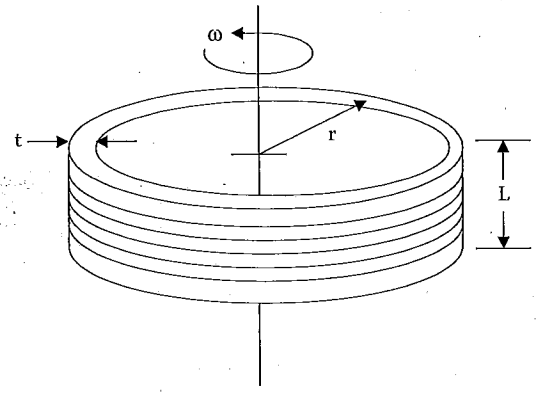

FIGURE 1.42
Simplified model of flywheel for problem 9.

the kinetic energy stored per unit mass of a ring made from 4340 steel with that of a ring made from IM-7 carbon fibers. For the carbon fiber ring, assume that the fibers are oriented in the circumferential direction, and that all of the tensile load is supported by the fibers.

References

1. Ashby, M.F. 1987. Technology of the 1990s: Advanced materials and predictive design. *Philosophical Transactions of the Royal Society of London*, A322, 393–407.
2. Wainwright, S.A., Biggs, W.D., Currey, J.D., and Gosline, J.M. 1976. *Mechanical Design in Organisms*. Princeton University Press, Princeton, NJ.
3. Griffith, A.A. 1920. The phenomena of rupture and flow in solids. *Philosophical Transactions of the Royal Society*, 221A, 163–198.
4. Gordon, J.E. 1976. *The New Science of Strong Materials*, 2nd ed. Princeton University Press, Princeton, NJ.
5. Thostenson, E.R., Ren, Z., and Chou, T.-W. 2001. Advances in the science and technology of carbon nanotubes and their composites: A review. *Composites Science and Technology*, 61, 1899–1912.
6. Qian, D., Wagner, J.G., Liu, W.K., Yu, M.F., and Ruoff, R.S. 2002. Mechanics of carbon nanotubes. *Applied Mechanics Reviews*, 55(6), 495–533.
7. McCrum, N.G., Buckley, C.P., and Bucknall, C.B. 1988. *Principles of Polymer Engineering*. Oxford University Press, New York.
8. Schwartz, M.M. 1984. *Composite Materials Handbook*. McGraw-Hill, Inc., New York.
9. Weeton, J.W., Peters, D.M., and Thomas, K.L. eds. 1987. *Engineer's Guide to Composite Materials*. ASM International, Materials Park, OH.
10. Lubin, G. ed. 1982. *Handbook of Composites*. Van Nostrand Reinhold Co., New York.
11. Katz, H.S. and Milewski, J.V. eds. 1978. *Handbook of Fillers and Reinforcements for Plastics*. Van Nostrand Reinhold Co., New York.
12. Reinhart, T.J. et al. eds. 1987. *Engineered Materials Handbook*, vol. 1, *Composites*. ASM International, Materials Park, OH.
13. Mallick, P.K. ed. 1997. *Composites Engineering Handbook*. Marcel Dekker, Inc., New York.
14. Harris, C.E., Starnes, J.H., Jr., and Shuart, M.J. 2001. *An Assessment of the State-of-the-Art in the Design and Manufacturing of Large Composite Structures for Aerospace Vehicles*. NASA TM-2001-210844.
15. Dexter, H.B. and Baker, D.J. 1994. Flight service environmental effects on composite materials and structures. *Advanced Performance Materials*, 1, 51–85.
16. Gibson, R.F., Suarez, S.A., and Deobald, L.R. 1985. Laboratory production of discontinuous-aligned fiber composite plates using an autoclave-style press cure. *Journal of Composites Technology and Research*, 7(2), 391–400.

17. Gutowski, T.G. ed. 1997. *Advanced Composites Manufacturing*. John Wiley & Sons, Inc., New York.
18. Crandall, S.H., Dahl, N.C., and Lardner, T.J. 1978. *An Introduction to the Mechanics of Solids* (2nd ed. with SI units). McGraw Hill, New York.
19. Riley, W.F., Sturges, L.D., and Morris, D.H. 2002. *Statics and Mechanics of Materials — An Integrated Approach*, 2nd ed. John Wiley & Sons, Inc., New York.

2

Lamina Stress–Strain Relationships

2.1 Introduction

The basic building block of a composite structure is the lamina, which usually consists of one of the fiber/matrix configurations shown in figure 1.4. For the purposes of mechanics analysis, however, the "unidirectionally reinforced" or "unidirectional" lamina with an arrangement of parallel, continuous fibers is the most convenient starting point. As shown in subsequent chapters, the stress–strain relationships for the unidirectional lamina form the basis for the analysis of not only the continuous fiber composite laminate (fig. 1.4[a]), but also of woven fiber (fig. 1.4[b]) and chopped fiber composites (fig. 1.4[c]) and (fig. 1.4[d]) as well.

A composite material is obviously heterogeneous at the constituent material level, with properties possibly changing from point to point. For example, the stress–strain relationships at a point are different for a point in the fiber material from how they are for a point in the matrix material. If we take the composite lamina as the basic building block, however, the "macromechanical" stress–strain relationships of the lamina can be expressed in terms of average stresses and strains and effective properties of an equivalent homogeneous material [1]. This chapter is concerned with the development and manipulation of these macromechanical stress–strain relationships. The "micromechanical" relationships between the constituent material properties and the effective lamina properties will be discussed in more detail in chapter 3, but the basic concept of an effective modulus will be discussed here.

To complicate matters further, the properties of a composite are usually anisotropic. That is, the properties associated with an axis passing through a point in the material generally depend on the orientation of the axis. By comparison, conventional metallic materials are nearly isotropic since their properties are essentially independent of orientation. Fortunately, each type of composite has characteristic material property symmetries that make it possible to simplify the general anisotropic stress–strain relationships. In particular, the symmetry possessed by the unidirectional lamina makes it a so-called orthotropic material. The symmetries associated with various types of composite laminae and the resulting lamina

stress–strain relationships are discussed in this chapter, along with certain mathematical manipulations that make it easier to deal with the directional nature of composite properties.

2.2 Effective Moduli in Stress–Strain Relationships

A general 3-D state of stress at a point in a material can be described by nine stress components σ_{ij} (where $i, j = 1, 2, 3$), as shown in figure 2.1. According to the conventional subscript notation, when $i = j$, the stress component σ_{ij} is a normal stress; and when $i \neq j$, the stress component is a shear stress. The first subscript refers to the *direction of the outward normal* to the face on which the stress component acts, and the second subscript refers to the direction in which the stress component itself acts.

Corresponding to each of the stress components, there is a strain component ε_{ij} describing the deformation at the point. Normal strains ($i = j$) describe the extension or contraction per unit length along the x_i direction, and shear strains ($i \neq j$) describe the distortional deformations associated with lines that were originally parallel to the x_i and x_j axes. It is very important to distinguish between the "tensor" strain ε_{ij} and the "engineering" strain γ_{ij}. In the case of normal strain, the engineering strain is the same as the tensor strain, but for shear strain $\varepsilon_{ij} = \gamma_{ij}/2$. Thus, the engineering shear strain γ_{ij} describes the total distortional change in the angle between

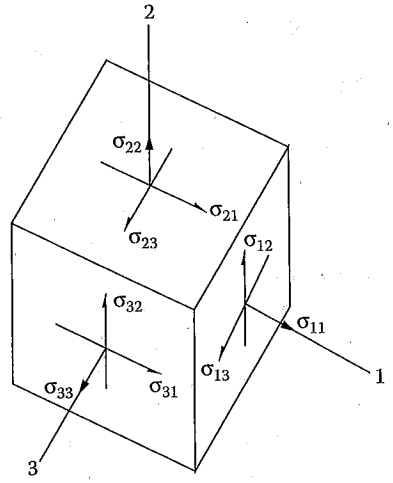

FIGURE 2.1
3-D state of stress

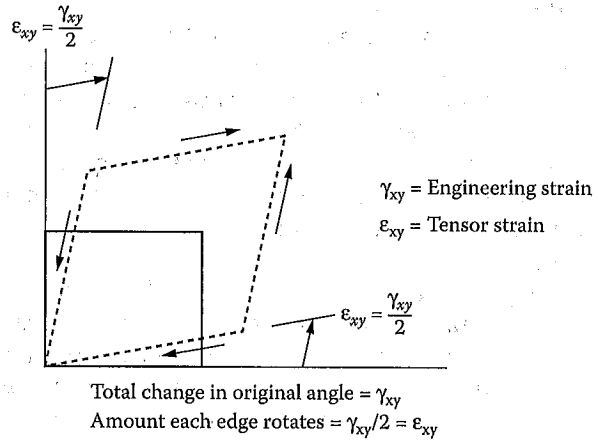

FIGURE 2.2
Geometric interpretation of engineering shear strain and tensor shear strain.

lines that were originally parallel to the x_i and x_j axes, but the tensor shear strain ε_{ij} describes the amount of rotation of either of the lines (fig. 2.2).

In the most general stress–strain relationship *at a point* in an elastic material each stress component is related to each of the nine strain components by an equation of the form

$$\sigma_{ij} = f_{ij}(\varepsilon_{11}, \varepsilon_{12}, \varepsilon_{13}, \varepsilon_{21}, \varepsilon_{22}, \varepsilon_{23}, \varepsilon_{31}, \varepsilon_{32}, \varepsilon_{33}) \tag{2.1}$$

where the functions f_{ij} may be nonlinear. For the linear elastic material, which is the primary concern in this book, the most general linear stress–strain relationships *at a point* in the material (excluding effects of environmental conditions) are given by equations of the form

$$\begin{Bmatrix} \sigma_{11} \\ \sigma_{22} \\ \sigma_{33} \\ \sigma_{23} \\ \sigma_{31} \\ \sigma_{12} \\ \sigma_{32} \\ \sigma_{13} \\ \sigma_{21} \end{Bmatrix} = \begin{bmatrix} C_{1111} & C_{1122} & C_{1133} & C_{1123} & C_{1131} & C_{1112} & C_{1132} & C_{1113} & C_{1121} \\ C_{2211} & C_{2222} & C_{2233} & C_{2223} & C_{2231} & C_{2212} & C_{2232} & C_{2213} & C_{2221} \\ C_{3311} & C_{3322} & C_{3333} & C_{3323} & C_{3331} & C_{3312} & C_{3332} & C_{3313} & C_{3321} \\ \cdots & \cdots & \cdots & \cdots & \cdots & \cdots & \cdots & \cdots & \cdots \\ \cdots & \cdots & \cdots & \cdots & \cdots & \cdots & \cdots & \cdots & \cdots \\ \cdots & \cdots & \cdots & \cdots & \cdots & \cdots & \cdots & \cdots & \cdots \\ \cdots & \cdots & \cdots & \cdots & \cdots & \cdots & \cdots & \cdots & \cdots \\ \cdots & \cdots & \cdots & \cdots & \cdots & \cdots & \cdots & \cdots & \cdots \\ C_{2111} & C_{2122} & C_{2133} & C_{2123} & C_{2131} & C_{2112} & C_{2132} & C_{2113} & C_{2121} \end{bmatrix} \begin{Bmatrix} \varepsilon_{11} \\ \varepsilon_{22} \\ \varepsilon_{33} \\ \varepsilon_{23} \\ \varepsilon_{31} \\ \varepsilon_{12} \\ \varepsilon_{32} \\ \varepsilon_{13} \\ \varepsilon_{21} \end{Bmatrix} \tag{2.2}$$

where [C] is a fully populated 9×9 matrix of stiffnesses or elastic constants (or moduli) having 81 components. Note that the first two subscripts on the elastic constants correspond to those of the stress, whereas the last two subscripts correspond to those of the strain. If no further restrictions are placed on the elastic constants, the material is called anisotropic and equation (2.2) is referred to as the generalized Hooke's law for anisotropic materials. In practice, there is no need to deal with this equation and its 81 elastic constants because various symmetry conditions simplify the equations considerably.

As shown in any mechanics of materials book [2], both stresses and strains are symmetric (i.e., $\sigma_{ij} = \sigma_{ji}$ and $\varepsilon_{ij} = \varepsilon_{ji}$), so that there are only six independent stress components and six independent strain components. This means that the elastic constants must be symmetric with respect to the first two subscripts and with respect to the last two subscripts (i.e., $C_{ijkl} = C_{jikl}$ and $C_{ijkl} = C_{ijlk}$ where $i, j, k, l = 1, 2, 3$), and that the number of nonzero elastic constants is now reduced to 36. These simplifications lead to a contracted notation that reduces the number of subscripts based on the following changes in notation [3–6]:

$$\sigma_{11} = \sigma_1 \qquad \varepsilon_{11} = \varepsilon_1$$

$$\sigma_{22} = \sigma_2 \qquad \varepsilon_{22} = \varepsilon_2$$

$$\sigma_{33} = \sigma_3 \qquad \varepsilon_{33} = \varepsilon_3$$

$$\sigma_{23} = \sigma_{32} = \sigma_4 \qquad 2\varepsilon_{23} = 2\varepsilon_{32} = \gamma_{23} = \gamma_{32} = \varepsilon_4$$

$$\sigma_{13} = \sigma_{31} = \sigma_5 \qquad 2\varepsilon_{13} = 2\varepsilon_{31} = \gamma_{13} = \gamma_{31} = \varepsilon_5$$

$$\sigma_{12} = \sigma_{21} = \sigma_6 \qquad 2\varepsilon_{12} = 2\varepsilon_{21} = \gamma_{12} = \gamma_{21} = \varepsilon_6$$

With this contracted notation, the generalized Hooke's law can now be written as

$$\sigma_i = C_{ij}\varepsilon_j, \quad i,j = 1,2,\ldots,6 \tag{2.3}$$

and the repeated subscript j implies summation on that subscript. Alternatively, in matrix form

$$\{\sigma\} = [C]\{\varepsilon\} \tag{2.4}$$

where the elastic constant matrix or stiffness matrix [C] is now 6×6 with 36 components and the stresses $\{\sigma\}$ and strains $\{\varepsilon\}$ are column vectors,

each having six elements. Alternatively, the generalized Hooke's law relating strains to stresses can be written as

$$\varepsilon_i = S_{ij}\sigma_j, \quad i,j = 1,2,\ldots,6 \tag{2.5}$$

or in matrix form as

$$\{\varepsilon\} = [S]\{\sigma\} \tag{2.6}$$

where [S] is the compliance matrix, which is the inverse of the stiffness matrix ($[S] = [C]^{-1}$). As shown later, due to the existence of the strain energy density, the stiffness and compliance matrices are symmetric. Note that nothing has been said thus far about any symmetry that the material itself may have. All real materials have some form of symmetry, however, and no known material is completely anisotropic.

Before discussing the various simplifications of the stress–strain relationships, it is appropriate to deal with the problem of heterogeneity in the composite material. Recall that the stress–strain relationships presented up to now are only valid *at a point* in the material, and that the stresses, strains, and elastic moduli will change as we move from point to point in a composite (i.e., the elastic moduli for the matrix material are different from those of the fiber). In order to analyze the macromechanical behavior of the composite, it is more convenient to deal with *averaged* stresses and strains that are related by "effective moduli" of an equivalent homogeneous material. Figure 2.3 shows schematically how the stresses in a heterogeneous composite may be nonuniform even though the imposed strain is uniform.

As shown in figure 2.3, if the scale of the inhomogeneity in a material can be characterized by some length dimension, d, then the length dimension, L, over which the macromechanical averaging is to take place, must be much larger than d if the average stresses and strains are to be related by effective moduli of an equivalent homogeneous material. We now define the average stresses, $\bar{\sigma}_i$, and the average strains, $\bar{\varepsilon}_i$, ($i = 1, 2,\ldots, 6$) to be averaged over a volume V, which is characterized by the dimension L, so that [1]

$$\bar{\sigma}_i = \int_V \sigma_i dv/V \tag{2.7}$$

$$\bar{\varepsilon}_i = \int_V \varepsilon_i dv/V \tag{2.8}$$

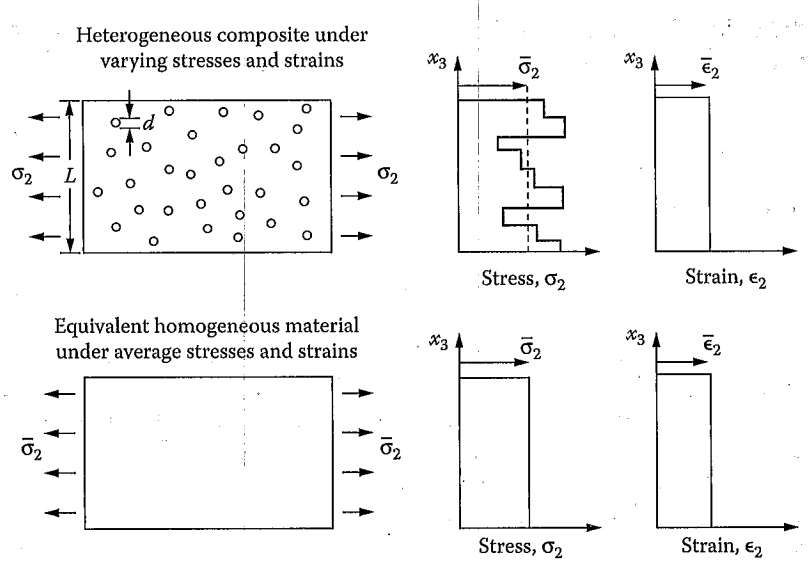

FIGURE 2.3
Concept of an effective modulus of an equivalent homogeneous material.

where $i = 1, 2, \ldots, 6$ and the σ_i, and the ε_i are the position-dependent stresses and strains at a point, respectively. If these averaged stresses and strains are used in place of the stresses and strains at a point, the generalized Hooke's law (i.e., eq. [2.3]) becomes

$$\bar{\sigma}_i = C_{ij}\bar{\varepsilon}_j \tag{2.9}$$

and the elastic moduli C_{ij} then become the "effective moduli" of the equivalent homogeneous material in volume V. Similarly, the "effective compliances" S_{ij} may be defined by

$$\bar{\varepsilon}_i = S_{ij}\bar{\sigma}_j \tag{2.10}$$

For example, in figure 2.3, the scale of the inhomogeneity is assumed to be the diameter of the fiber, d, and the averaging dimension, L, is assumed to be a characteristic lamina dimension such that $L \gg d$. The effective modulus C_{22} of the lamina is thus defined as $C_{22} = \bar{\sigma}_2/\bar{\varepsilon}_2$. In the remainder of this book, lamina properties are assumed to be effective properties as described above.

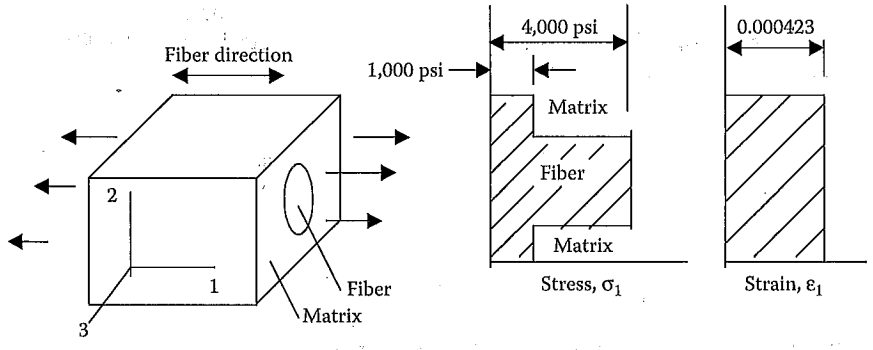

FIGURE 2.4
Stress and strain distributions for calculation of effective modulus in example 2.1.

EXAMPLE 2.1

A representative volume element (RVE) from a fiber-reinforced composite lamina is shown in figure 2.4, along with the longitudinal stress and strain distributions across the fiber and matrix materials in the section. The fiber has a uniform longitudinal stress of 4000 psi (along the 1 direction) and a diameter of 0.0003 in., while the matrix has a uniform longitudinal stress of 1000 psi. A uniform longitudinal strain of 0.000423 in./in. acts over the entire section. The RVE has edge dimensions 0.0004 in. × 0.0004 in. in the 23 plane. Assume that the cross-sectional dimensions of the section do not change along the longitudinal direction, and use the concept of the effective modulus of an equivalent homogeneous material to find the numerical value of the effective longitudinal modulus, E_1 (or E_{11}) of the composite.

Solution. The effective longitudinal modulus is given by

$$E_1 = \frac{\bar{\sigma}_1}{\bar{\varepsilon}_1}$$

where the average stress is

$$\bar{\sigma}_1 = \frac{\int \sigma_1 dV}{\int dV} = \frac{\int \sigma_1 dA}{\int dA} = \frac{\sigma_f A_f + \sigma_m A_m}{A_f + A_m}$$

$$= \frac{(4000)\frac{\pi}{4}(0.0003)^2 + (1000)[(0.0004)^2 - \frac{\pi}{4}(0.0003)^2]}{(0.0004)^2} = 2325 \text{ psi}$$

and the stresses and cross-sectional areas of the fiber and matrix are denoted by the subscripts f and m, respectively. The average strain is $\bar{\varepsilon}_1 = 0.000423$, so the effective modulus is

$$E_1 = \frac{\bar{\sigma}_1}{\bar{\varepsilon}_1} = \frac{2325}{0.000423} = 5.496(10^6)\text{psi}$$

2.3 Symmetry in Stress–Strain Relationships

In this section, the generalized anisotropic Hooke's law will be simplified and specialized using various symmetry conditions. The first symmetry condition, which has nothing to do with material symmetry, is strictly a result of the existence of a strain energy density function [3,6]. The strain energy density function, W, is such that the stresses can be derived according to the equation

$$\sigma_i = \frac{\partial W}{\partial \varepsilon_i} = C_{ij}\varepsilon_j \tag{2.11}$$

where

$$W = \frac{1}{2} C_{ij}\varepsilon_i\varepsilon_j \tag{2.12}$$

By taking a second derivative of W, we find that

$$\frac{\partial^2 W}{\partial \varepsilon_i \partial \varepsilon_j} = C_{ij} \tag{2.13}$$

and by reversing the order of differentiation, we find that

$$\frac{\partial^2 W}{\partial \varepsilon_j \partial \varepsilon_i} = C_{ji} \tag{2.14}$$

Since the result must be the same regardless of the order of the differentiation, $C_{ij} = C_{ji}$, the stiffness matrix is symmetric. Similarly, W can be expressed in terms of compliances and stresses, and by taking two derivatives with respect to stresses, it can be shown that $S_{ij} = S_{ji}$. Thus, the compliance matrix is also symmetric. Due to these mathematical manipulations,

only 21 of the 36 anisotropic elastic moduli or compliances are independent, and we still have not said anything about any inherent symmetry of the material itself.

According to the above developments, the stiffness matrix for the linear elastic anisotropic material without any material property symmetry is of the form

$$C_{ij} = \begin{bmatrix} C_{11} & C_{12} & C_{13} & C_{14} & C_{15} & C_{16} \\ & C_{22} & C_{23} & C_{24} & C_{25} & C_{26} \\ & & C_{33} & C_{34} & C_{35} & C_{36} \\ & \text{SYM} & & C_{44} & C_{45} & C_{46} \\ & & & & C_{55} & C_{56} \\ & & & & & C_{66} \end{bmatrix} \tag{2.15}$$

Further simplifications of the stiffness matrix are possible only if the material properties have some form of symmetry. For example, a *monoclinic* material has one plane of material property symmetry. It can be shown [3,7] that since the C_{ij} for such a material must be invariant under a transformation of coordinates corresponding to reflection in the plane of symmetry, the number of independent elastic constants for the monoclinic material is reduced to 13. Such a symmetry condition is generally not of practical interest in composite material analysis, however.

As shown in figure 2.5, a unidirectional composite lamina has three mutually orthogonal planes of material property symmetry (i.e., the 12,

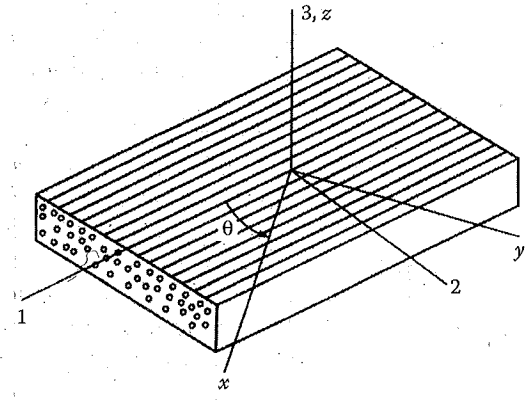

FIGURE 2.5
Orthotropic lamina with principal (123) and nonprincipal (xyz) coordinate systems.

23, and 13 planes) and is called an *orthotropic* material. The term "orthotropic" alone is not sufficient to describe the form of the stiffness matrix, however. Unlike the anisotropic stiffness matrix (eq. [2.15]), which has the same form (but different terms) for different coordinate systems, the form of the stiffness matrix for the orthotropic material depends on the coordinate system used. The 123 coordinate axes in figure 2.5 are referred to as the *principal material coordinates* since they are associated with the reinforcement directions. Invariance of the C_{ij} under transformations of coordinates corresponding to reflections in two orthogonal planes [3,7] may be used to show that the stiffness matrix for a so-called *specially orthotropic* material associated with the principal material coordinates is of the form

$$C_{ij} = \begin{bmatrix} C_{11} & C_{12} & C_{13} & 0 & 0 & 0 \\ & C_{22} & C_{23} & 0 & 0 & 0 \\ & & C_{33} & 0 & 0 & 0 \\ & \text{SYM} & & C_{44} & 0 & 0 \\ & & & & C_{55} & 0 \\ & & & & & C_{66} \end{bmatrix} \tag{2.16}$$

A stiffness matrix of this form in terms of engineering constants will be obtained in the next section using observations from simple experiments. Note that there are only 12 nonzero elastic constants and 9 independent elastic constants for the specially orthotropic material.

Table 2.1 summarizes similar results for the different combinations of materials and coordinate systems used in this book. It will also be shown later that if the stress–strain relationships for the same orthotropic material are developed for a nonprincipal coordinate system *xyz* as shown in figure 2.5, the stiffness matrix is of the same form as that of the anisotropic material in equation (2.15). In such a nonprincipal or off-axis coordinate system, the material is called *generally orthotropic* (table 2.1). There are two other types of material symmetry that are important in the study of composites. The details will be developed in the next section, but the general forms of the stiffness matrices are given here for completeness. In most composites the fiber-packing arrangement is statistically random in nature, so that the properties are nearly the same in any direction perpendicular to the fibers (i.e., that properties along the 2 direction are the same as those along the 3 direction), and the material is *transversely isotropic*. For such a material we would expect that $C_{22} = C_{33}$, $C_{12} = C_{13}$, $C_{55} = C_{66}$, and that C_{44} would not be independent

TABLE 2.1

Elastic Coefficients in the Stress–Strain Relationships for Different Materials and Coordinate Systems

Material and Coordinate System	Number of Nonzero Coefficients	Number of Independent Coefficients
3-D Case		
Anisotropic	36	21
Generally orthotropic (nonprincipal coordinates)	36	9
Specially orthotropic (principal coordinates)	12	9
Specially orthotropic, transversely isotropic	12	5
Isotropic	12	2
2-D Case (Lamina)		
Anisotropic	9	6
Generally orthotropic (nonprincipal coordinates)	9	4
Specially orthotropic (principal coordinates)	5	4
Balanced orthotropic, or square symmetric (principal coordinates)	5	3
Isotropic	5	2

from the other stiffnesses. It can be shown [1] that the complete stiffness matrix for a specially orthotropic, transversely isotropic material is of the form

$$C_{ij} = \begin{bmatrix} C_{11} & C_{12} & C_{12} & 0 & 0 & 0 \\ & C_{22} & C_{23} & 0 & 0 & 0 \\ & & C_{22} & 0 & 0 & 0 \\ & \text{SYM} & & (C_{22} - C_{23})/2 & 0 & 0 \\ & & & & C_{66} & 0 \\ & & & & & C_{66} \end{bmatrix} \tag{2.17}$$

where the 23 plane and all parallel planes are assumed to be planes of isotropy. In the next section, a stiffness matrix of the same form will be derived, except that the so-called *engineering constants* will be used instead

of the C_{ij}. Note that now there are still 12 nonzero elastic moduli but that only 5 are independent (table 2.1).

The simplest form of the stress–strain relationship occurs when the material is *isotropic* and every coordinate axis is an axis of symmetry. Now we would expect that $C_{11} = C_{22} = C_{33}$, $C_{12} = C_{13} = C_{23}$, that $C_{44} = C_{55} = C_{66}$, and that C_{44} again would not be independent from the other C_{ij}. The isotropic stiffness matrix is of the form [1]

$$C_{ij} = \begin{bmatrix} C_{11} & C_{12} & C_{12} & 0 & 0 & 0 \\ & C_{11} & C_{12} & 0 & 0 & 0 \\ & & C_{11} & 0 & 0 & 0 \\ & \text{SYM} & & (C_{11}-C_{12})/2 & 0 & 0 \\ & & & & (C_{11}-C_{12})/2 & 0 \\ & & & & & (C_{11}-C_{12})/2 \end{bmatrix} \tag{2.18}$$

Now there are still 12 nonzero elastic constants, but only 2 are independent (table 2.1). Similar equations based on the engineering constants will be derived in the next section. Equations of this form can be found in any mechanics of materials book, and the design of metallic components is usually based on such formulations.

2.4 Orthotropic and Isotropic Engineering Constants

In the previous section, symmetry conditions were shown to reduce the number of elastic constants (the C_{ij} or S_{ij}) in the stress–strain relationships for several important classes of materials and the general forms of the relationships were presented. When a material is characterized experimentally, however, the so-called "engineering constants" such as Young's modulus (or modulus of elasticity), shear modulus, and Poisson's ratio are usually measured instead of the C_{ij} or the S_{ij}. The engineering constants are also widely used in analysis and design because they are easily defined and interpreted in terms of simple states of stress and strain. In this section, several simple tests and their resulting states of stress and strain will be used to develop the 3-D and 2-D stress–strain relationships for orthotropic and isotropic materials.

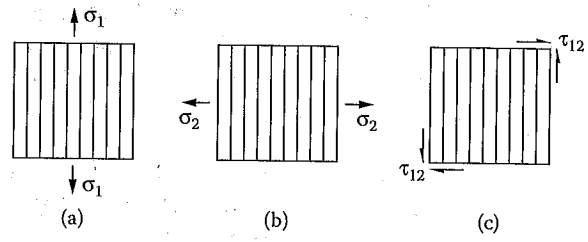

FIGURE 2.6
Simple states of stress used to define lamina engineering constants.

Consider a simple uniaxial tensile test consisting of an applied longitudinal normal stress, σ_1, along the reinforcement direction (i.e., the 1 direction) of a specimen from an orthotropic material, as shown in figure 2.6(a). It is assumed that all other stresses are equal to zero. Within the linear range the experimental observation is that the resulting strains associated with the 123 axes can be expressed empirically in terms of "engineering constants" as

$$\begin{aligned} \varepsilon_1 &= \sigma_1 / E_1 \\ \varepsilon_2 &= -\nu_{12}\varepsilon_1 = -\nu_{12}\sigma_1 / E_1 \\ \varepsilon_3 &= -\nu_{13}\varepsilon_1 = -\nu_{13}\sigma_1 / E_1 \\ \gamma_{12} &= \gamma_{23} = \gamma_{13} = 0 \end{aligned} \tag{2.19}$$

where E_1 = longitudinal modulus of elasticity associated with the 1 direction, and $\nu_{ij} = \varepsilon_j/\varepsilon_i$ is the Poisson's ratio, the ratio of the strain in the j direction to the strain in the perpendicular i direction when the applied stress is in the i direction.

Recall from mechanics of materials [2] that for isotropic materials no subscripts are needed on properties such as the modulus of elasticity and the Poisson's ratio because the properties are the same in all directions. This is not the case with orthotropic materials, however, and subscripts are needed on these properties because of their directional nature. For example, $E_1 \neq E_2$ and $\nu_{12} \neq \nu_{21}$. Note that, as with isotropic materials, a negative sign must be used in the definition of Poisson's ratio. A property like ν_{12} is usually called a *major Poisson's ratio*, whereas a property like ν_{21} is called a *minor Poisson's ratio*. As with isotropic materials, a normal

stress induces only normal strains, and all shear strains are equal to zero. This lack of shear/normal interaction is observed only for the principal material coordinate system, however. For any other set of coordinates the so-called "shear-coupling" effect is present. This effect will be discussed in more detail later.

Now consider a similar experiment where a transverse normal stress, σ_2, is applied to the same material as shown in figure 2.6(b), with all other stresses being equal to zero. Now the experimental observation is that the resulting strains can be expressed as

$$\begin{aligned} \varepsilon_2 &= \sigma_2 / E_2 \\ \varepsilon_1 &= -\nu_{21}\varepsilon_2 = -\nu_{21}\sigma_2 / E_2 \\ \varepsilon_3 &= -\nu_{23}\varepsilon_2 = -\nu_{23}\sigma_2 / E_2 \\ \gamma_{12} &= \gamma_{23} = \gamma_{13} = 0 \end{aligned} \tag{2.20}$$

where E_2 is the transverse modulus of elasticity associated with the 2 direction. A similar result for an applied transverse normal stress, σ_3, can be obtained by changing the appropriate subscripts in equation (2.20).

Next, consider a shear test where a pure shear stress, $\sigma_{12} = \tau_{12}$, is applied to the material in the 12 plane, as shown in figure 2.6(c). Now the experimental observation is that resulting strains can be written as

$$\begin{aligned} \gamma_{12} &= \tau_{12} / G_{12} \\ \varepsilon_1 &= \varepsilon_2 = \varepsilon_3 = \gamma_{13} = \gamma_{23} = 0 \end{aligned} \tag{2.21}$$

where G_{12} is the shear modulus associated with the 12 plane. Similar results can be obtained for pure shear in the 13 and 23 planes by changing the appropriate subscripts in equation (2.21). Again, notice that there is no shear/normal interaction (or shear coupling). As before, however, this is only true for the principal material axes.

Finally, consider a general 3-D state of stress consisting of all possible normal and shear stresses associated with the 123 axes as shown in figure 2.1. Since we are dealing with linear behavior, it is appropriate to use superposition and add all the resulting strains due to the simple uniaxial and shear tests, as given in equation (2.19), equation (2.20),

equation (2.21), and similar equations as described above. The resulting set of equations is given below:

$$\begin{Bmatrix} \varepsilon_1 \\ \varepsilon_2 \\ \varepsilon_3 \\ \gamma_{23} \\ \gamma_{31} \\ \gamma_{12} \end{Bmatrix} = \begin{bmatrix} 1/E_1 & -\nu_{21}/E_2 & -\nu_{31}/E_3 & 0 & 0 & 0 \\ -\nu_{12}/E_1 & 1/E_2 & -\nu_{32}/E_3 & 0 & 0 & 0 \\ -\nu_{13}/E_1 & -\nu_{23}/E_2 & 1/E_3 & 0 & 0 & 0 \\ 0 & 0 & 0 & 1/G_{23} & 0 & 0 \\ 0 & 0 & 0 & 0 & 1/G_{31} & 0 \\ 0 & 0 & 0 & 0 & 0 & 1/G_{12} \end{bmatrix} \begin{Bmatrix} \sigma_1 \\ \sigma_2 \\ \sigma_3 \\ \tau_{23} \\ \tau_{31} \\ \tau_{12} \end{Bmatrix} \tag{2.22}$$

Note that the compliance matrix is of the same form as the stiffness matrix for a specially orthotropic material (eq. [2.16]) as it should be because $[S] = [C]^{-1}$. Note also that due to symmetry of the compliance matrix, $\nu_{ij}/E_i = \nu_{ji}/E_j$ and only nine of the engineering constants are independent.

If we now consider a simple uniaxial tensile test consisting of an applied normal stress, σ_x, along some arbitrary x axis as shown in figure 2.5 we find that the full complement of normal strains and shear strains are developed. The generation of shear strains due to normal stresses and normal strains due to shear stresses is often referred to as the "shear-coupling effect." As a result of shear coupling, all the zeros disappear in the compliance matrix and it becomes fully populated for the general 3-D state of stress associated with the arbitrary xyz axes; this is the *generally orthotropic* material. The stiffness or compliance matrices for the generally orthotropic material are of the same form as those for the general anisotropic material (eq. [2.15]), although the material still has its orthotropic symmetries with respect to the principal material axes. Obviously then, the experimental characterization of such a material is greatly simplified by testing it as a specially orthotropic material along the principal material directions. As shown later, once we have the stiffnesses or compliances associated with the 123 axes, we can obtain those for an arbitrary off-axis coordinate system such as xyz by transformation equations involving the angles between the axes.

If the material being tested is specially orthotropic and transversely isotropic, the subscripts 2 and 3 in equations (2.22) are interchangeable, and we have $G_{13} = G_{12}$, $E_2 = E_3$, $\nu_{21} = \nu_{31}$, and $\nu_{23} = \nu_{32}$. In addition, the familiar relationship among the isotropic engineering constants [2] is now valid for the engineering constants associated with the 23 plane, so that

$$G_{23} = \frac{E_2}{2(1+\nu_{32})} \tag{2.23}$$

Now the compliance matrix is of the same form as equation (2.17) and only five of the engineering constants are independent.

Finally, for the isotropic material there is no need for subscripts and $G_{13} = G_{23} = G_{12} = G$, $E_1 = E_2 = E_3 = E$, $\nu_{12} = \nu_{23} = \nu_{13} = \nu$, and $G = E/2(1 + \nu)$. Now the compliance matrix is of the same form as equation (2.18) and only two of the engineering constants are independent.

2.5 The Specially Orthotropic Lamina

As shown later in the analysis of laminates, the lamina is often assumed to be in a simple 2-D state of stress (or plane stress). In this case the specially orthotropic stress–strain relationships in equations (2.22) can be simplified by letting $\sigma_3 = \tau_{23} = \tau_{31} = 0$, so that

$$\begin{Bmatrix} \varepsilon_1 \\ \varepsilon_2 \\ \gamma_{12} \end{Bmatrix} = \begin{bmatrix} S_{11} & S_{12} & 0 \\ S_{21} & S_{22} & 0 \\ 0 & 0 & S_{66} \end{bmatrix} \begin{Bmatrix} \sigma_1 \\ \sigma_2 \\ \tau_{12} \end{Bmatrix} \tag{2.24}$$

where the compliances S_{ij} and the engineering constants are related by the equations

$$\begin{aligned} S_{11} &= \frac{1}{E_1}, \quad S_{22} = \frac{1}{E_2}, \\ S_{12} &= S_{21} = -\frac{\nu_{21}}{E_2} = -\frac{\nu_{12}}{E_1}, \quad S_{66} = \frac{1}{G_{12}} \end{aligned} \tag{2.25}$$

Thus, there are five nonzero compliances and only four independent compliances for the specially orthotropic lamina (table 2.1). The lamina stresses in terms of *tensor* strains are given by

$$\begin{Bmatrix} \sigma_1 \\ \sigma_2 \\ \tau_{12} \end{Bmatrix} = \begin{bmatrix} Q_{11} & Q_{12} & 0 \\ Q_{21} & Q_{22} & 0 \\ 0 & 0 & 2Q_{66} \end{bmatrix} \begin{Bmatrix} \varepsilon_1 \\ \varepsilon_2 \\ \gamma_{12}/2 \end{Bmatrix} \tag{2.26}$$

where the Q_{ij} are the components of the lamina stiffness matrix, which are related to the compliances and the engineering constants by

$$\begin{aligned} Q_{11} &= \frac{S_{22}}{S_{11}S_{22} - S_{12}^2} = \frac{E_1}{1 - \nu_{12}\nu_{21}} \\ Q_{12} &= \frac{S_{12}}{S_{11}S_{22} - S_{12}^2} = \frac{\nu_{12}E_2}{1 - \nu_{12}\nu_{21}} = Q_{21} \\ Q_{22} &= \frac{S_{11}}{S_{11}S_{22} - S_{12}^2} = \frac{E_2}{1 - \nu_{12}\nu_{21}} \\ Q_{66} &= \frac{1}{S_{66}} = G_{12} \end{aligned} \tag{2.27}$$

Note that the factor of 2 has been introduced in the Q_{66} term of equation (2.26) to compensate for the use of tensor shear strain $\varepsilon_{12} = \gamma_{12}/2$. The reason for this will become apparent in the next section. As shown later, the experimental characterization of the orthotropic lamina involves the measurement of four independent engineering constants such as E_1, E_2, G_{12}, and ν_{12}. Typical values of these properties for several composites are shown in table 2.2.

The balanced orthotropic lamina shown schematically in figure 2.7 often occurs in practice when the fiber reinforcement is woven or cross-plied at 0° and 90°. In this case the number of independent elastic constants in equations (2.24) to equation (2.27) is reduced to 3 because of the double symmetry of properties with respect to the 1 and 2 axes (table 2.1).

Thus, for the balanced orthotropic lamina, we have $E_1 = E_2$, $Q_{11} = Q_{22}$, and $S_{11} = S_{22}$.

2.6 The Generally Orthotropic Lamina

In the analysis of laminates having multiple laminae, it is often necessary to know the stress–strain relationships for the *generally orthotropic lamina* in nonprincipal coordinates (or "off-axis" coordinates) such as x and y in figure 2.5. Fortunately, the elastic constants in these so-called "off-axis" stress–strain relationships are related to the four independent elastic constants in the principal material coordinates and the lamina orientation angle. The sign convention for the lamina orientation angle, θ, is given in figure 2.8. The relationships are found by combining the equations for transformation of stress and strain components from the 12 axes to the xy axes.

TABLE 2.2

Typical Values of Lamina Engineering Constants for Several Composites Having Fiber Volume Fraction v_f

Material	E_1 (Msi [GPa])	E_2 (Msi [GPa])	G_{12} (Msi [GPa])	ν_{12}	v_f
T300/934 carbon/epoxy	19.0 (131)	1.5 (10.3)	1.0 (6.9)	0.22	0.65
AS/3501 carbon/epoxy	20.0 (138)	1.3 (9.0)	1.0 (6.9)	0.3	0.65
P-100/ERL 1962 pitch/ carbon/epoxy	68.0 (468.9)	0.9 (6.2)	0.81 (5.58)	0.31	0.62
IM7/8551-7 carbon/ toughened epoxy	23.5(162)	1.21(8.34)	0.3(2.07)	0.34	0.6
AS4/APC2 carbon/ PEEK	19.1(131)	1.26(8.7)	0.73(5.0)	0.28	0.58
Boron/6061 boron/ aluminum	34.1(235)	19.9(137)	6.8(47.0)	0.3	0.5
Kevlar® 49/934 aramid/ epoxy	11.0 (75.8)	0.8 (5.5)	0.33 (2.3)	0.34	0.65
Scotchply® 1002 E-glass/epoxy	5.6 (38.6)	1.2 (8.27)	0.6 (4.14)	0.26	0.45
Boron/5505 boron/ epoxy	29.6 (204.0)	2.68 (18.5)	0.81 (5.59)	0.23	0.5
Spectra® 900/826 polyethylene/epoxy	4.45 (30.7)	0.51 (3.52)	0.21 (1.45)	0.32	0.65
E-glass/470-36 E-glass/vinylester	3.54 (24.4)	1.0 (6.87)	0.42 (2.89)	0.32	0.30

Kevlar® is a registered trademark of DuPont Company, Wilmington, Delaware; Scotchply® is a registered trademark of 3M Company, St. Paul, Minnesota; and Spectra® is a registered trademark of Honeywell International, Inc.

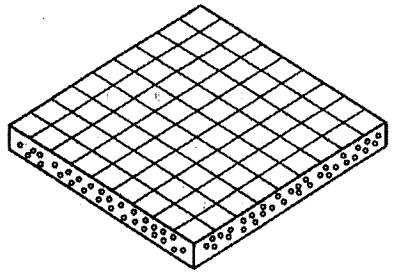

FIGURE 2.7
Balanced orthotropic lamina consisting of fibers oriented at 0° and 90°.

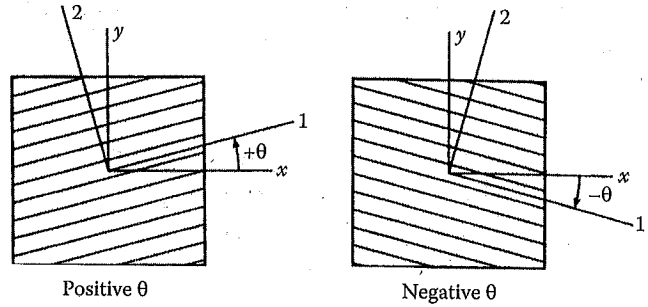

FIGURE 2.8
Sign convention for lamina orientation.

Relationships for transformation of stress components between coordinate axes may be obtained by writing the equations of static equilibrium for the wedge-shaped differential element in figure 2.9. For example, the force equilibrium along the x direction is given by

$$\sum F_x = \sigma_x dA - \sigma_1 dA \cos^2\theta - \sigma_2 dA \sin^2\theta + 2\tau_{12} dA \sin\theta \cos\theta = 0 \tag{2.28}$$

which, after dividing through by dA, gives an equation relating σ_x to the stresses in the 12 system:

$$\sigma_x = \sigma_1 \cos^2\theta + \sigma_2 \sin^2\theta - 2\tau_{12} \sin\theta \cos\theta \tag{2.29}$$

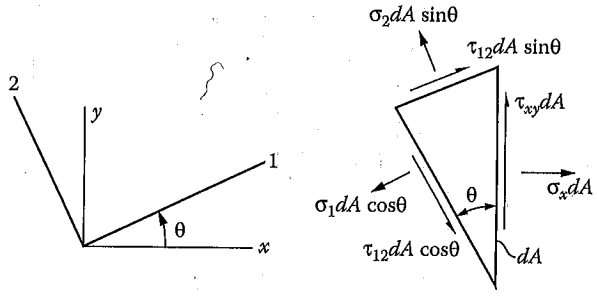

FIGURE 2.9
Differential element under static equilibrium with forces in two coordinate systems.

Using a similar approach, the complete set of transformation equations for the stresses in the xy-coordinate system can be developed and written in matrix form as

$$\begin{Bmatrix}\sigma_x\\ \sigma_y\\ \tau_{xy}\end{Bmatrix}=\begin{bmatrix}c^2 & s^2 & -2cs\\ s^2 & c^2 & 2cs\\ cs & -cs & c^2-s^2\end{bmatrix}\begin{Bmatrix}\sigma_1\\ \sigma_2\\ \tau_{12}\end{Bmatrix}=[T]^{-1}\begin{Bmatrix}\sigma_1\\ \sigma_2\\ \tau_{12}\end{Bmatrix} \tag{2.30}$$

and the stresses in the 12 system can be written as

$$\begin{Bmatrix}\sigma_1\\ \sigma_2\\ \tau_{12}\end{Bmatrix}=[T]\begin{Bmatrix}\sigma_x\\ \sigma_y\\ \tau_{xy}\end{Bmatrix} \tag{2.31}$$

where $c = \cos\theta$, $s = \sin\theta$, and the transformation matrix, $[T]$, is defined as

$$[T]=\begin{bmatrix}c^2 & s^2 & 2cs\\ s^2 & c^2 & -2cs\\ -cs & cs & c^2-s^2\end{bmatrix} \tag{2.32}$$

Methods for determining the matrix inverse $[T]^{-1}$ are described in any book dealing with matrices. It can also be shown [2,3] that the *tensor strains* transform the same way as the stresses, and that

$$\begin{Bmatrix}\varepsilon_1\\ \varepsilon_2\\ \gamma_{12}/2\end{Bmatrix}=[T]\begin{Bmatrix}\varepsilon_x\\ \varepsilon_y\\ \gamma_{xy}/2\end{Bmatrix} \tag{2.33}$$

Substituting equation (2.33) into equation (2.26), and then substituting the resulting equations into equations (2.30), we find that

$$\begin{Bmatrix}\sigma_x\\ \sigma_y\\ \tau_{xy}\end{Bmatrix}=[T]^{-1}[Q][T]\begin{Bmatrix}\varepsilon_x\\ \varepsilon_y\\ \gamma_{xy}/2\end{Bmatrix} \tag{2.34}$$

where the stiffness matrix $[Q]$ in equations (2.34) is defined in equations (2.26)

Carrying out the indicated matrix multiplications and converting back to engineering strains, we find that

$$\begin{Bmatrix}\sigma_x\\ \sigma_y\\ \tau_{xy}\end{Bmatrix}=\begin{bmatrix}\bar{Q}_{11} & \bar{Q}_{12} & \bar{Q}_{16}\\ \bar{Q}_{12} & \bar{Q}_{22} & \bar{Q}_{26}\\ \bar{Q}_{16} & \bar{Q}_{26} & \bar{Q}_{66}\end{bmatrix}\begin{Bmatrix}\varepsilon_x\\ \varepsilon_y\\ \gamma_{xy}\end{Bmatrix} \tag{2.35}$$

where the $\bar{Q}_{ij}$ are the components of the transformed lamina stiffness matrix which are defined as follows:

$$\begin{aligned}
\bar{Q}_{11} &= Q_{11}\cos^4\theta + Q_{22}\sin^4\theta + 2(Q_{12}+2Q_{66})\sin^2\theta\cos^2\theta\\
\bar{Q}_{12} &= (Q_{11}+Q_{22}-4Q_{66})\sin^2\theta\cos^2\theta + Q_{12}(\cos^4\theta+\sin^4\theta)\\
\bar{Q}_{22} &= Q_{11}\sin^4\theta + Q_{22}\cos^4\theta + 2(Q_{12}+2Q_{66})\sin^2\theta\cos^2\theta\\
\bar{Q}_{16} &= (Q_{11}-Q_{12}-2Q_{66})\cos^3\theta\sin\theta - (Q_{22}-Q_{12}-2Q_{66})\cos\theta\sin^3\theta\\
\bar{Q}_{26} &= (Q_{11}-Q_{12}-2Q_{66})\cos\theta\sin^3\theta - (Q_{22}-Q_{12}-2Q_{66})\cos^3\theta\sin\theta\\
\bar{Q}_{66} &= (Q_{11}+Q_{22}-2Q_{12}-2Q_{66})\sin^2\theta\cos^2\theta + Q_{66}(\sin^4\theta+\cos^4\theta)
\end{aligned} \tag{2.36}$$

Although the transformed lamina stiffness matrix now has the same form as that of an anisotropic material with nine nonzero coefficients, only four of the coefficients are independent because they can all be expressed in terms of the four independent lamina stiffnesses of the specially orthotropic material. That is, the material is still orthotropic, but it is not recognizable as such in the off-axis coordinates. As in the 3-D case, it is obviously much easier to characterize the lamina experimentally in the principal material coordinates than in the off-axis coordinates. Recall that the engineering constants, the properties that are normally measured, are related to the lamina stiffnesses by equations (2.27).

Alternatively, the strains can be expressed in terms of the stresses as

$$\begin{Bmatrix}\varepsilon_x\\ \varepsilon_y\\ \gamma_{xy}\end{Bmatrix}=\begin{bmatrix}\bar{S}_{11} & \bar{S}_{12} & \bar{S}_{16}\\ \bar{S}_{12} & \bar{S}_{22} & \bar{S}_{26}\\ \bar{S}_{16} & \bar{S}_{26} & \bar{S}_{66}\end{bmatrix}\begin{Bmatrix}\sigma_x\\ \sigma_y\\ \tau_{xy}\end{Bmatrix} \tag{2.37}$$

where the $\bar{S}_{ij}$ are the components of the transformed lamina compliance matrix that are defined by equations similar to, but not exactly the same form as, equations (2.36)

The lamina engineering constants can also be transformed from the principal material axes to the off-axis coordinates. For example, the off-axis modulus of elasticity associated with uniaxial loading the x direction is defined as

$$E_x = \frac{\sigma_x}{\varepsilon_x} = \frac{\sigma_x}{\bar{S}_{11}\sigma_x} = \frac{1}{\bar{S}_{11}} \tag{2.38}$$

where the strain ε_x in the denominator has been found by substituting the stress conditions $\sigma_x \neq 0$, $\sigma_y = \tau_{xy} = 0$ in equations (2.37). By replacing $\bar{S}_{11}$ with an equation similar to the first of equations (2.36) and then using equations (2.25), we get the first of equation (2.39):

$$\begin{aligned}
E_x &= \left[\frac{1}{E_1}c^4 + \left(\frac{1}{G_{12}} - \frac{2\nu_{12}}{E_1}\right)s^2c^2 + \frac{1}{E_2}s^4\right]^{-1} \\
E_y &= \left[\frac{1}{E_1}s^4 + \left(\frac{1}{G_{12}} - \frac{2\nu_{12}}{E_1}\right)s^2c^2 + \frac{1}{E_2}c^4\right]^{-1} \\
G_{xy} &= \left[\frac{1}{G_{12}}(s^4 + c^4) + 4\left(\frac{1}{E_1} + \frac{1}{E_2} + \frac{2\nu_{12}}{E_1} - \frac{1}{2G_{12}}\right)s^2c^2\right]^{-1} \\
\nu_{xy} &= E_x\left[\frac{\nu_{12}}{E_1}(s^4 + c^4) - \left(\frac{1}{E_1} + \frac{1}{E_2} - \frac{1}{G_{12}}\right)s^2c^2\right]
\end{aligned} \tag{2.39}$$

where $c = \cos\theta$ and $s = \sin\theta$ as before.

The variation of these properties with lamina orientation for several composites is shown graphically in figure 2.10 from ref. [8]. As intuitively expected, E_x varies from a maximum at $\theta = 0°$ to a minimum at $\theta = 90°$ for this particular material. It is not necessarily true that the extreme values of such material properties occur along the principal material directions, however [6]. What may not be intuitively expected is the sharp drop in modulus as the angle changes slightly from 0° and the fact that over much of the range of lamina orientations the modulus is very low. This is why transverse reinforcement is needed in most composites.

The shear-coupling effect has been described previously as the generation of shear strains by off-axis normal stresses and the generation of normal strains by off-axis shear stresses. One way to quantify the degree of shear coupling is by defining dimensionless shear-coupling ratios [4,5]

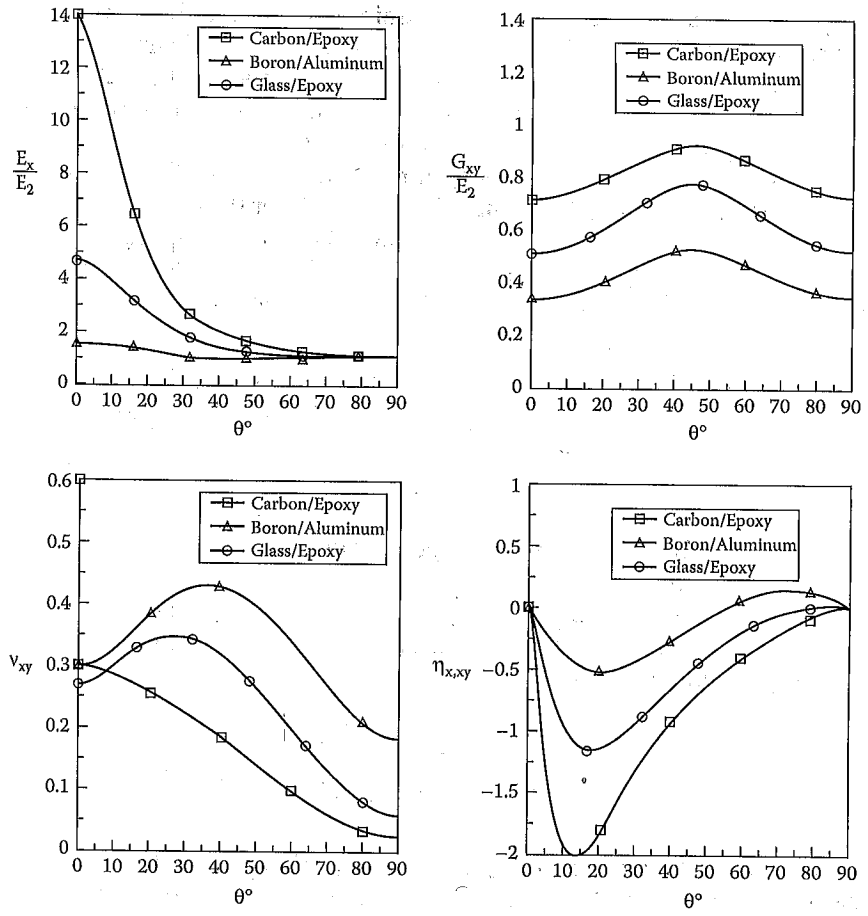

FIGURE 2.10
Variations of off-axis engineering constants with lamina orientation for carbon/epoxy, boron/aluminum and glass/epoxy composites. (From Sun, C.T. 1998. *Mechanics of Aircraft Structures*. John Wiley & Sons, New York. With permission.)

or mutual influence coefficients [9] or shear-coupling coefficients [10]. For example, when the state of stress is defined as $\sigma_x \neq 0$, $\sigma_y = \tau_{xy} = 0$, the ratio

$$\eta_{x,xy} = \frac{\gamma_{xy}}{\varepsilon_x} = \frac{\bar{S}_{16}}{\bar{S}_{11}} = E_x\left[\left(\frac{2}{E_1} + \frac{2\nu_{12}}{E_1} - \frac{1}{G_{12}}\right)sc^3 - \left(\frac{2}{E_2} + \frac{2\nu_{12}}{E_1} - \frac{1}{G_{12}}\right)s^3c\right] \tag{2.40}$$

is a measure of the amount of shear strain generated in the xy plane per unit normal strain along the direction of the applied normal stress, σ_x. Thus, the shear-coupling ratio is analogous to the Poisson's ratio, which is a measure of the coupling between normal strains. As shown in figure 2.10, $\eta_{x,xy}$ strongly depends on orientation and has its maximum value at some intermediate angle which depends on the material. Since there is no coupling along principal material directions, $\eta_{x,xy} = 0$ for $\theta = 0°$ and $\theta = 90°$. As the shear-coupling ratio increases, the amount of shear coupling increases. Other shear-coupling ratios can be defined for different states of stress. For example, when the stresses are $\tau_{xy} \neq 0$, $\sigma_x = \sigma_y = 0$, the ratio

$$\eta_{xy,y} = \frac{\varepsilon_y}{\gamma_{xy}} = \frac{\bar{S}_{26}}{\bar{S}_{66}} = G_{xy}\left[\left(\frac{2}{E_1} + \frac{2\nu_{12}}{E_1} - \frac{1}{G_{12}}\right)s^3c - \left(\frac{2}{E_2} + \frac{2\nu_{12}}{E_1} - \frac{1}{G_{12}}\right)sc^3\right] \tag{2.41}$$

characterizes the normal strain response along the y direction due to a shear stress in the xy plane.

Finally, for a generally orthotropic lamina under plane stress, the stress–strain relationship for the normal strain ε_x in terms of off-axis engineering constants can be expressed as:

$$\varepsilon_x = \frac{1}{E_x}\sigma_x - \frac{\nu_{yx}}{E_y}\sigma_y + \frac{\eta_{xy,x}}{G_{xy}}\tau_{xy} \tag{2.42}$$

with similar relationships for ε_y and γ_{xy}. As with the specially orthotropic case and the general anisotropic case, the stiffness and compliance matrices are still symmetric. So, for example, the off-axis compliances $\bar{S}_{12} = \bar{S}_{21}$, or in terms of off-axis engineering constants, $\frac{\nu_{yx}}{E_y} = \frac{\nu_{xy}}{E_x}$.

EXAMPLE 2.2

A 45° off-axis tensile test is conducted on a generally orthotropic test specimen by applying a normal stress σ_x as shown in figure 2.11. The specimen has strain gages attached so as to measure the normal strains ε_x and ε_y along the x and y directions, respectively. How many engineering constants for this material can be determined from the measured parameters σ_x, ε_x, and ε_y?

Solution. The off-axis modulus of elasticity along the x direction is determined from

$$E_x = \frac{\sigma_x}{\varepsilon_x}$$

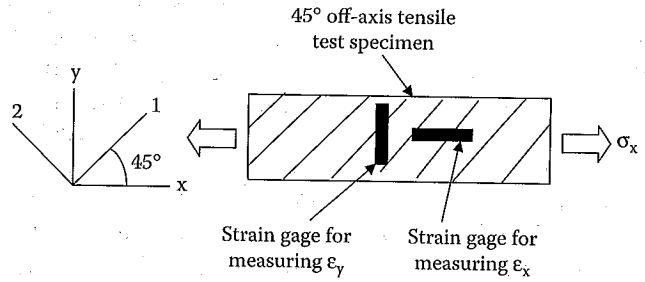

FIGURE 2.11
Strain-gaged specimen for a 45° off-axis tensile test.

The off-axis major Poisson's ratio is given by

$$\nu_{xy} = -\frac{\varepsilon_y}{\varepsilon_x}$$

Although it may not be obvious at first glance, the in-plane shear modulus G_{12} may also be found from these measurements by using the appropriate transformation equations for stress and strain. Using $\theta = 45°$ in equation (2.33), the shear strain γ_{12} is found from

$$\frac{\gamma_{12}}{2} = -\cos 45° \sin 45° \varepsilon_x + \cos 45° \sin 45° \varepsilon_y + (\cos^2 45° - \sin^2 45°)\frac{\gamma_{xy}}{2}$$

or

$$\gamma_{12} = -\varepsilon_x + \varepsilon_y$$

Note that the γ_{xy} term drops out of the above equation only when $\theta = 45°$. For any other value of θ, we would need to know γ_{xy} as well as ε_x and ε_y in order to find γ_{12} from this transformation equation. Likewise, the shear stress τ_{12} is found by substituting the tensile test conditions $\sigma_x \neq 0$, $\sigma_y = \tau_{xy} = 0$ in equation (2.31):

$$\tau_{12} = -\cos 45° \sin 45° \sigma_x = -\frac{\sigma_x}{2}$$

Finally, the shear modulus G_{12} is given in terms of the measured parameters as

$$G_{12} = \frac{\tau_{12}}{} = \frac{\sigma_x}{}$$

The effects of lamina orientation on stiffness are difficult to assess from inspection of stiffness transformation equations such as equations (2.36) and equation (2.39). In addition, the eventual incorporation of lamina stiffnesses into laminate analysis requires integration of lamina stiffnesses over the laminate thickness, and integration of such complicated equations is also difficult. In view of these difficulties, a more convenient "invariant" form of the lamina stiffness transformation equations has been proposed by Tsai and Pagano [11]. By using trigonometric identities to convert from power functions to multiple angle functions and then using additional mathematical manipulations, Tsai and Pagano showed that equations (2.36) could also be written as

$$\begin{aligned}
\bar{Q}_{11} &= U_1 + U_2\cos 2\theta + U_3\cos 4\theta \\
\bar{Q}_{12} &= U_4 - U_3\cos 4\theta \\
\bar{Q}_{22} &= U_1 - U_2\cos 2\theta + U_3\cos 4\theta \\
\bar{Q}_{16} &= \frac{U_2}{2}\sin 2\theta + U_3\sin 4\theta \\
\bar{Q}_{26} &= \frac{U_2}{2}\sin 2\theta - U_3\sin 4\theta \\
\bar{Q}_{66} &= \frac{1}{2}(U_1 - U_4) - U_3\cos 4\theta
\end{aligned} \tag{2.43}$$

where the set of "invariants" is defined as

$$\begin{aligned}
U_1 &= \frac{1}{8}(3Q_{11} + 3Q_{22} + 2Q_{12} + 4Q_{66}) \\
U_2 &= \frac{1}{2}(Q_{11} - Q_{22}) \\
U_3 &= \frac{1}{8}(Q_{11} + Q_{22} - 2Q_{12} - 4Q_{66}) \\
U_4 &= \frac{1}{8}(Q_{11} + Q_{22} + 6Q_{12} - 4Q_{66})
\end{aligned} \tag{2.44}$$

As the name implies, the invariants, which are simply linear combinations of the Q_{ij}, are invariant to rotations in the plane of the lamina. Note that there are four independent invariants, just as there are four independent

elastic constants. Equation (2.43) is obviously easier to manipulate and interpret than equations (2.36). For example, all the stiffness expressions except those for the coupling stiffnesses consist of one constant term and terms that vary with lamina orientation. Thus, the effects of lamina orientation on stiffness are easier to interpret.

Invariant formulations of lamina compliance transformations are also useful. It can be shown [5,10] that the off-axis compliance components in equation (2.37) can be written as

$$\begin{aligned}
\bar{S}_{11} &= V_1 + V_2\cos 2\theta + V_3\cos 4\theta \\
\bar{S}_{12} &= V_4 - V_3\cos 4\theta \\
\bar{S}_{22} &= V_1 - V_2\cos 2\theta + V_3\cos 4\theta \\
\bar{S}_{16} &= V_2\sin 2\theta + 2V_3\sin 4\theta \\
\bar{S}_{26} &= V_2\sin 2\theta - 2V_3\sin 4\theta \\
\bar{S}_{66} &= 2(V_1 - V_4) - 4V_3\cos 4\theta
\end{aligned} \tag{2.45}$$

where the invariants are

$$\begin{aligned}
V_1 &= \frac{1}{8}(3S_{11} + 3S_{22} + 2S_{12} + S_{66}) \\
V_2 &= \frac{1}{2}(S_{11} - S_{22}) \\
V_3 &= \frac{1}{8}(S_{11} + S_{22} - 2S_{12} - S_{66}) \\
V_4 &= \frac{1}{8}(S_{11} + S_{22} + 6S_{12} - S_{66})
\end{aligned} \tag{2.46}$$

Invariant formulations also lend themselves well to graphical interpretation. As shown in any mechanics of materials book [2], stress transformation equations such as equations (2.30) can be combined and manipulated so as to generate the equation of Mohr's circle. As shown in figure 2.12, the transformation of a normal stress component σ_x can be described by the invariant formulation

$$\sigma_x = I_1 + I_2\cos 2\theta_p \tag{2.47}$$

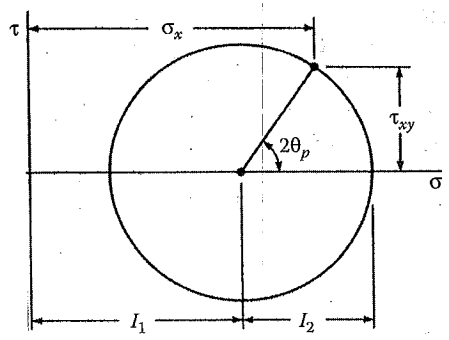

FIGURE 2.12
Mohr's circle for stress transformation.

$$\text{where } I_1 = \frac{\sigma_x + \sigma_y}{2} = \text{invariant}$$

$$I_2 = \sqrt{\left[\frac{\sigma_x - \sigma_y}{2}\right]^2 + \tau_{xy}^2} = \text{invariant}$$

θ_p = angle between the x axis and the principal stress axis

In this case the invariants are I_1, which defines the position of the center of the circle, and I_2, which is the radius of the circle. Note that, as with equation (2.43), the invariant formulation typically consists of a constant term and a term that varies with orientation. Similarly, the invariant forms of the stiffness transformations can also be interpreted graphically using Mohr's circles. For example, Tsai and Hahn [10] have shown that the stiffness transformation equation

$$\bar{Q}_{11} = U_1 + U_2 \cos 2\theta + U_3 \cos 4\theta \tag{2.48}$$

can be represented graphically by using two Mohr's circles, as shown in figure 2.13. The distance between points on each of the two circles represents the total stiffness $\bar{Q}_{11}$, whereas the distance between the centers of the two circles is given by U_1. The radius and angle associated with one circle are U_2 and 2θ, respectively, and the radius and angle associated with the other circle are U_3 and 4θ, respectively. Thus, the distance between the centers of the circles is a measure of the isotropic component of stiffness, whereas the radii of the circles indicate the strength of the orthotropic component. If $U_2 = U_3 = 0$, the circles collapse to points and the material is isotropic.

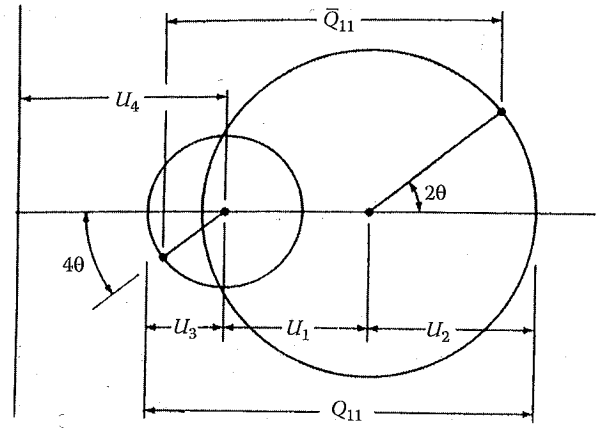

FIGURE 2.13
Mohr's circles for stiffness transformation. (From Tsai, S.W. and Hahn, H.T. 1980. *Introduction to Composite Materials*. Technomic Publishing Co., Lancaster, PA. Reprinted by permission of Technomic Publishing Co.)

Invariants will prove to be very useful later in the analysis of randomly oriented short fiber composites and laminated plates. For additional applications of invariants in composite analysis, the reader is referred to books by Halpin [5] and Tsai and Hahn [10].

EXAMPLE 2.3

A filament wound cylindrical pressure vessel (fig. 2.14) of mean diameter $d = 1$ m and wall thickness $t = 20$ mm is subjected to an internal pressure, p. The filament winding angle $\theta = 53.1°$ from the longitudinal axis of the pressure vessel, and the glass/epoxy material has the following properties: $E_1 = 40$ GPa $= 40(10^3)$ MPa, $E_2 = 10$ GPa, $G_{12} = 3.5$ GPa, and $\nu_{12} = 0.25$. By the use of a strain gage, the normal strain along the fiber direction is determined to be $\varepsilon_1 = 0.001$. Determine the internal pressure in the vessel.

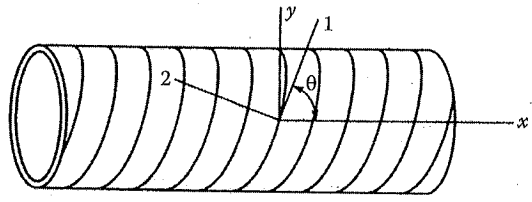

FIGURE 2.14
Filament wound vessel.

Solution. From mechanics of materials, the stresses in a thin-walled cylindrical pressure vessel are given by

$$\sigma_x = \frac{pr}{2t} = \frac{0.5p}{2(0.02)} = 12.5p, \quad \tau_{xy} = 0$$

$$\sigma_y = \frac{pr}{t} = \frac{0.5p}{0.02} = 25p$$

(Note that $r = d/2 = 0.5$ m.)

These equations are based on static equilibrium and geometry only. Thus, they apply to a vessel made of any material. Since the given strain is along the fiber direction, we must transform the above stresses to the 12 axes. Recall that in the "netting analysis" in problem 5 and problem 6 of chapter 1 only the fiber longitudinal normal stress was considered. This was because the matrix was ignored, and the fibers alone cannot support transverse or shear stresses. In the current problem, however, the transverse normal stress, σ_2, and the shear stress, τ_{12}, are also considered because the fiber and matrix are now assumed to act as a composite. From equations (2.31), the stresses along the 12 axes are

$$\sigma_1 = \sigma_x \cos^2\theta + \sigma_y \sin^2\theta + 2\tau_{xy}\sin\theta\cos\theta$$
$$= (12.5p)(0.6)^2 + (25p)(0.8)^2 + 0 = 20.5p(\text{MPa})$$
$$\sigma_2 = \sigma_x \sin^2\theta + \sigma_y \cos^2\theta - 2\tau_{xy}\sin\theta\cos\theta$$
$$= (12.5p)(0.8)^2 + (25p)(0.6)^2 - 0 = 17.0p(\text{MPa})$$
$$\tau_{12} = -\sigma_x \sin\theta\cos\theta + \sigma_y \sin\theta\cos\theta + \tau_{xy}(\cos^2\theta - \sin^2\theta)$$
$$= -(12.5p)(0.8)(0.6) + (25p)(0.6)(0.8) + 0 = 6.0p(\text{MPa})$$

where the pressure p is in MPa. From the first of equations (2.24), the normal strain ε_1 is

$$\varepsilon_1 = \frac{\sigma_1}{E_1} - \frac{\nu_{12}\sigma_2}{E_1} = \frac{20.5p}{40(10^3)} - \frac{0.25(17.0p)}{40(10^3)} = 0.001$$

and the resulting pressure is $p = 2.46$ MPa.

EXAMPLE 2.4

A tensile test specimen is cut out along the x direction of the pressure vessel described in example 2.3. What effective modulus of elasticity would you expect to get during a test of this specimen?

Solution. The modulus of elasticity, E_x, associated with the x direction is given by the first of equations (2.39) with $\theta = 53.1°$.

$$E_x = \frac{1}{\frac{1}{E_1}c^4 + \left[-\frac{2\nu_{12}}{E_1} + \frac{1}{G_{12}}\right]c^2s^2 + \frac{1}{E_2}s^4}$$

$$E_x = \frac{1}{\frac{1}{40}(0.6)^4 + \left[-\frac{2(0.25)}{40} + \frac{1}{3.5}\right](0.6)^2(0.8)^2 + \frac{1}{10}(0.8)^4} = 9.33 \text{ GPa}$$

EXAMPLE 2.5

A lamina consisting of continuous fibers randomly oriented in the plane of the lamina is said to be "planar isotropic," and the elastic properties in the plane are isotropic in nature. Find expressions for the lamina stiffnesses for a planar isotropic lamina.

Solution. Since the fibers are assumed to be randomly oriented in the plane, the "planar isotropic stiffnesses" can be found by averaging the transformed lamina stiffnesses as follows:

$$\tilde{Q}_{ij} = \frac{\int_0^\pi \bar{Q}_{ij}\,d\theta}{\int_0^\pi d\theta}$$

where the superscript (~) denotes an averaged property.

It is convenient to use the invariant forms of the transformed lamina stiffnesses because they are easily integrated. For example, if we substitute the first of equations (2.43) in the above equation, we get

$$\tilde{Q}_{11} = \frac{\int_0^\pi \bar{Q}_{11}d\theta}{\int_0^\pi d\theta} = \frac{\int_0^\pi [U_1 + U_2\cos 2\theta + U_3\cos 4\theta]d\theta}{\pi} = U_1$$

Note that the averaged stiffness equals the isotropic part of the transformed lamina stiffness, and that the orthotropic parts drop out in the averaging process. Similarly, the other averaged stiffnesses can be found in terms of the invariants. The derivations of the remaining expressions are left as an exercise.

2.7 Problems

1. A representative section from a composite lamina is shown in figure 2.15 along with the transverse stress and strain distributions across the fiber and matrix materials in the section. Assuming that the dimensions of the section do not change along the longitudinal direction (perpendicular to the page), find the numerical value of the effective transverse modulus for the section.
2. Derive the first of equations (2.39) for the off-axis modulus, E_x.
3. Derive the third of equations (2.39) for the off-axis shear modulus, G_{xy}.
4. Using the result from problem 3:
   (a) Find the value of the angle θ (other than 0° or 90°) where the curve of G_{xy} vs. θ has a possible maximum, minimum, or inflection point.
   (b) For the value of θ found in part (a), find the bounds on G_{12} which must be satisfied if G_{xy} is to have a maximum or minimum.
   (c) Qualitatively sketch the variation of G_{xy} vs. θ for the different cases and identify each curve by the corresponding bounds on G_{12}, which give that curve.
   (d) Using the bounds on G_{12} from part (b), find which conditions apply for E-glass/epoxy composites. The bounds on G_{12} in part (b) should be expressed in terms of E_1, E_2, and ν_{12}.

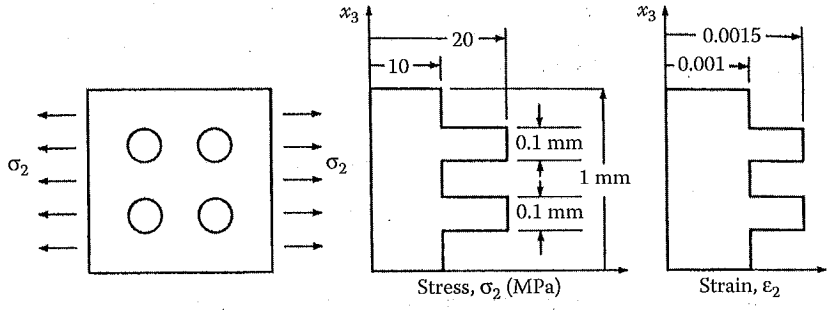

FIGURE 2.15
Transverse stress and strain distribution over a section of lamina.

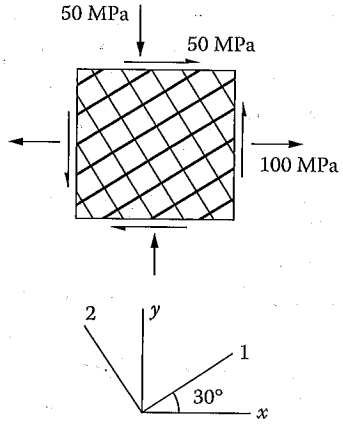

FIGURE 2.16
Stresses acting on an element of balanced orthotropic lamina.

5. Describe a series of tensile tests that could be used to measure the four independent engineering constants for an orthotropic lamina without using a pure shear test. Give the necessary equations for the data reduction.
6. A balanced orthotropic, or square symmetric lamina, is made up of 0° and 90° fibers woven into a fabric and bonded together, as shown in figure 2.7.
   (a) Describe the stress–strain relationships for such a lamina in terms of the appropriate engineering constants.
   (b) For a typical glass/epoxy composite lamina of this type, sketch the expected variations of all the engineering constants for the lamina from 0° to 90°. Numerical values are not required.
7. An element of a balanced orthotropic carbon/epoxy lamina is under the state of stress shown in figure 2.16. If the properties of the woven carbon fabric/epoxy material are $E_1 = 70$ GPa, $\nu_{12} = 0.25$, $G_{12} = 5$ GPa, determine all the strains along the fiber directions.
8. Derive equations (2.27).
9. Express the stress–strain relationships in equations (2.37) in terms of off-axis engineering constants such as the moduli of elasticity, shear modulus, Poisson's ratios, and shear-coupling ratios.

10. Derive the first two equations of equations (2.43).
11. Find all components of the stiffness and compliance matrices for a specially orthotropic lamina made of AS/3501 carbon/epoxy.
12. Using the results of problem 11, determine the invariants U_i and V_i for the AS/3501 lamina, where $i = 1, 2, 3, 4$.
13. Using the results of problem 11 or problem 12, compare the transformed lamina stiffnesses for AS/3501 carbon/epoxy plies oriented at +45° and 45°.
14. Show how the Mohr's circles in figure 2.13 can be used to interpret the transformed lamina stiffness $\bar{Q}_{12}$.
15. Using the approach described in example 2.5, derive the expressions for all the averaged stiffnesses for the planar isotropic lamina in terms of invariants. Use these results to find the corresponding averaged engineering constants (modulus of elasticity, shear modulus, and Poisson's ratio) in terms of invariants.
16. For a specially orthotropic, transversely isotropic material the "plane strain bulk modulus," K_{23}, is an engineering constant that is defined by the stress conditions $\sigma_2 = \sigma_3 = \sigma$ and the strain conditions $\varepsilon_1 = 0$, $\varepsilon_2 = \varepsilon_3 = \varepsilon$. Show that these conditions lead to the stress–strain relationship $\sigma = 2K_{23}\varepsilon$, and find the relationship among K_{23}, E_1, E_2, G_{23}, and ν_{12}.
17. Describe the measurements that would have to be taken and the equations that would have to be used to determine G_{23}, ν_{32}, and E_2 for a specially orthotropic, transversely isotropic material from a single tensile test.
18. A 45° off-axis tensile test specimen has three strain gages attached. Two of the gages are mounted as shown in figure 2.11 so as to measure the normal strains ε_x and ε_y, and a third gage is mounted at $\theta = 45°$ so as to measure the normal strain ε_1. If the applied stress $\sigma_x = 100$ MPa and the measured strains are $\varepsilon_x = 0.00647$, $\varepsilon_y = -0.00324$ and $\varepsilon_1 = 0.00809$, determine the off-axis modulus of elasticity E_x, the off-axis major Poisson's ratio ν_{xy} and the shear coupling ratio $\eta_{x,xy}$.

References

1. Christensen, R.M. 1979. *Mechanics of Composite Materials*. John Wiley & Sons, New York.
2. Crandall, S.H., Dahl, N.C., and Lardner, T.J. 1978. *An Introduction to the Mechanics of Solids* (2d ed. with SI units). McGraw-Hill, Inc., New York.

3. Sokolnikoff, I.S. 1956. *Mathematical Theory of Elasticity*. McGraw-Hill, Inc., New York.
4. Ashton, J.E., Halpin, J.C., and Petit, P.H. 1969. *Primer on Composite Materials: Analysis*. Technomic Publishing Co., Lancaster, PA.
5. Halpin, J.C. 1984. *Primer on Composite Materials: Analysis*, rev. ed. Technomic Publishing Co., Lancaster, PA.
6. Jones, R.M. 1999. *Mechanics of Composite Materials Second Edition*. Taylor and Francis, Inc., Philadelphia, PA.
7. Vinson, J.R. and Sierakowski, R.L. 1986. *The Behavior of Structures Composed of Composite Materials*. Martinus Nijhoff Publishers, Dordrecht, The Netherlands.
8. Sun, C.T. 1998. *Mechanics of Aircraft Structures*. John Wiley & Sons, New York.
9. Lekhnitski, S.G. 1981. *Theory of Elasticity of an Anisotropic Body*. Mir Publishing Co., Moscow, USSR.
10. Tsai, S.W. and Hahn, H.T. 1980. *Introduction to Composite Materials*. Technomic Publishing Co., Lancaster, PA.
11. Tsai, S.W. and Pagano, N.J. 1968. Invariant properties of composite materials, in Tsai, S.W., Halpin, J.C., and Pagano N.J. eds., *Composite Materials Workshop*, pp. 233–253. Technomic Publishing Co., Lancaster, PA.